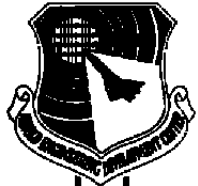# Contamination Effects of Satellite Material Outgassing Products on Thermal Surfaces and Solar Cells

B. L. Seiber, W. T. Bertrand,
and
B. E. Wood
Calspan Corporation/AEDC Operations

December 1990

Final Report for Period October 1, 1988 through September 30, 1990

**ARNOLD ENGINEERING DEVELOPMENT CENTER
ARNOLD AIR FORCE BASE, TENNESSEE
AIR FORCE SYSTEMS COMMAND
UNITED STATES AIR FORCE**

This report has been reviewed by the Office of Public Affairs (PA) and is releasable to the National Technical Information Service (NTIS). At NTIS, it will be available to the general public, including foreign nations.

APPROVAL STATEMENT

This report has been reviewed and approved.

SETH SHEPHERD, Capt, USAF
Flight Dynamics Division
Directorate of Technology
Deputy for Operations

Approved for publication:

FOR THE COMMANDER

KEITH L. KUSHMAN
Technical Director
Directorate of Technology
Deputy for Operations

REPORT DOCUMENTATION PAGE

Public reporting burden for this collection of information is estimated to average 1 hour per response, including the time for reviewing instructions, searching existing data sources, gathering and maintaining the data needed, and completing and reviewing the collection of information. Send comments regarding this burden estimate or any other aspect of this collection of information, including suggestions for reducing this burden, to Washington Headquarters Services, Directorate for Information Operations and Reports, 1215 Jefferson Davis Highway, Suite 1204, Arlington, VA 22202-4302, and to the Office of Management and Budget, Paperwork Reduction Project (0704-0188), Washington, DC 20503

1 AGENCY USE ONLY (Leave blank)	2 REPORT DATE December 1990	3 REPORT TYPE AND DATES COVERED Final, 10/1/88 - 9/30/90	
4 TITLE AND SUBTITLE **Contamination Effects of Satellite Material Outgassing Products on Thermal Control Surfaces and Solar Cells**			5 FUNDING NUMBERS **PE - 92102F**
6 AUTHOR(S) **Seiber, B. L., Bertrand, W. T., and Wood, B. E., Calspan Corporation/AEDC Operations**			
7 PERFORMING ORGANIZATION NAME(S) AND ADDRESS(ES) **Arnold Engineering Development Center/DOF** **Air Force Systems Command** **Arnold Air Force Base, Tennessee 37389-5000**			8 PERFORMING ORGANIZATION REPORT NUMBER **AEDC-TR-90-27**
9 SPONSORING/MONITORING AGENCY NAMES(S) AND ADDRESS(ES) **Air Force Wright Research and Development Center** **Wright-Patterson Air Force Base, Ohio 45433**			10 SPONSORING/MONITORING AGENCY REPORT NUMBER
11 SUPPLEMENTARY NOTES **Available in Defense Technical Information Center (DTIC).**			
12a DISTRIBUTION/AVAILABILITY STATEMENT **Approved for public release; distribution is unlimited.**			12b DISTRIBUTION CODE

13 ABSTRACT (Maximum 200 words)

The Wright Research and Development Center (WRDC) and the Arnold Engineering Development Center (AEDC) have initiated a program for measuring optical and radiative effects of satellite material outgassing products on thermal control and cryo-optic surfaces. A solar absorptance chamber for making reflectance/absorptance measurements on thermal control materials has been established. This report describes the operation of the solar absorptance chamber used to measure the degradation of reflective surfaces and solar cells caused by deposition of outgassing contaminants. The effects of solar irradiation (UV) were also studied, and results are presented. Data are presented for Dow Corning 93-500 Space-grade encapsulant (DC93-500), Furane Products Uralane® 5753-A/B(LV) encapsulant, and Polyclad FR-4 Epoxy® laminate.

14. SUBJECT TERMS solar absorptance material outgassing effects reflectance			15 NUMBER OF PAGES **57**
			16 PRICE CODE
17 SECURITY CLASSIFICATION OF REPORT **UNCLASSIFIED**	18 SECURITY CLASSIFICATION OF THIS PAGE **UNCLASSIFIED**	19 SECURITY CLASSIFICATION OF ABSTRACT **UNCLASSIFIED**	20 LIMITATION OF ABSTRACT **SAME AS REPORT**

COMPUTER GENERATED

PREFACE

The work reported herein was performed by the Arnold Engineering Development Center (AEDC), Air Force Systems Command (AFSC). The results were obtained by Calspan Corporation, AEDC Operations, operating contractor for aerospace flight dynamics testing at AEDC, AFSC, Arnold Air Force Base, Tennessee, under AEDC Project Number DB72VW (V32K-CT). The project was sponsored by the Wright Research and Development Center (WRDC), Wright-Patterson AFB, Ohio. The WRDC Project Manager was Capt. Arthur Estavillo, and the AEDC Project Manager was Capt. Seth Shepherd/DOF. The manuscript was submitted for publication on November 28, 1990.

The authors would like to thank Bill Hobbs, Winfred Johnson, and L. E. Phillips for their help with the Solar Absorptance Measurements (SAM) Chamber operation and instrumentation; John Henry Jones for the spectrometer data acquisition program; Earl Kiech for the absorptance calculations; and R. J. Bryson for effusion cell calculations.

CONTENTS

ILLUSTRATIONS

1.0 INTRODUCTION

As satellite applications become more sophisticated and satellite lifetimes are extended, the roles of contamination prediction and control become increasingly important. Contamination can end a mission because of cryogenically cooled optical systems becoming coated or thermal control surfaces becoming contaminated, thereby increasing the solar absorptance and causing the spacecraft to overheat. These are the two most important ways contamination can adversely affect the mission.

A spacecraft designer must predict effects of contamination with a very limited amount of data. Previously, the ASTM E 595 (Ref. 1) has been the industry standard for screening materials. The total mass loss (TML) and the collected volatile condensable material (CVCM) are used as guides. From the ASTM E 595 criteria, to be space-rated, a material must have a TML of less than 1 percent and a CVCM of less than 0.1 percent. These parameters are determined by heating a sample to 125°C for 24 hr under vacuum. The TML is found from the measurements of the sample weight before and after heating. The CVCM is determined by weighing a 25°C collector surface that was positioned above the heated sample before and after the 24-hr heating cycle. Neither the time history, nor the identification of outgassed species, are available from the ASTM E 595 test.

The Wright Research and Development Center (WRDC) is pursuing a plan to determine the outgassing properties of materials and the effects of condensed gases on critical surfaces such as thermal control and cryogenically cooled optical components. An improved test method for determining material outgassing characteristics has been developed by Lockheed (Ref. 2). This method uses quartz crystal microbalances (QCMs) maintained at 77 to 298 K to measure the mass loss by outgassing, and a time history of each outgassed species. This test method can be used to indicate how much of a given satellite material may be lost in space by outgassing, but it cannot determine what effect the outgassed material will have on an optical or thermal radiative surface. The surface effects of these products are being studied at the Arnold Engineering Development Center (AEDC) under another program sponsored by WRDC (Ref. 3).

The Solar Absorptance Measurements (SAM) Chamber was built to investigate the effects of solar radiation upon contaminant films. It has been shown that the ultraviolet portion of the solar radiation causes changes in the contaminant film absorptance (Ref. 4), but more information is desired. There are two basic classes of contaminant sources, silicones and organics. For this study, Dow Corning 93-500 space-grade encapsulant (DC93-500), a silicone, and Furane Products Uralane® 5753—A/B (LV) urethane casting compound and electrical insulation (Uralane), an organic, were chosen. In addition, Polyclad FR-4 Epoxy® laminate was studied for the Massachusetts Institute of Technology Lincoln Laboratory (MIT/LL).

The primary goal of this work was to obtain the absorptance change on an aluminum mirror with contaminant thickness and to obtain the absorptance change with solar irradiation time. The spectral absorptance measurements were made over the wavelength range from 250 to 2,300 nm, where 95 percent of the solar energy is concentrated. Because the samples were nontransmitting, the spectral absorptance, $a(\lambda)$, can be determined from $1 - r(\lambda)$, where $r(\lambda)$ is the spectral reflectance. The spectral reflectance was actually the quantity measured.

The approach was to condense a contaminant layer on an aluminum mirror under vacuum and measure the change in reflectance with contaminant film thickness *in situ*. Then, the contaminated mirror was irradiated under vacuum with an xenon solar lamp, and the change in reflectance with solar irradiation time was measured. This procedure was repeated for another mirror with a different thickness of the contaminant.

An additional goal of this study was to observe solar cell degradation under contamination followed by solar irradiation. Contaminant deposition procedures on the solar cell were similar to that previously described for the mirrors. Silicon and gallium arsenide solar cells were obtained from WRDC and mounted on an aluminum panel in the SAM Chamber. The change in the outputs of the solar cells with contaminant thickness was initially recorded. The solar cells were then irradiated with the xenon solar lamp, and their outputs were measured as the contaminant film degraded with lamp exposure time. The contaminant chosen for these studies was the Dow Corning 93-500 space-grade encapsulant.

2.0 EXPERIMENTAL TEST APPARATUS

2.1 SOLAR ABSORPTANCE MEASUREMENTS CHAMBER

The solar absorptance measurements (SAM) chamber provides a technique for measuring changes in the absorption of solar radiation by thermal control or optical surfaces contaminated by outgassing products at vacuum conditions. The equipment also allows generation of the outgassing products within the chamber and the determination of the amount of material deposited on the sample surface using a QCM. If desired, the condensed outgassing products can be irradiated by simulated solar radiation after deposition. For the current measurements, a contaminant layer was deposited, and the layer was then irradiated. The chamber and associated contamination equipment are shown in Fig.1. The details of each of these systems are discussed separately in the following sections.

The SAM Chamber vacuum is maintained by a 360-ℓ/sec turbomolecular pump. The chamber is also outfitted with a liquid nitrogen cooled liner that can be used when test conditions dictate; however, this liner was not cooled for the measurements reported herein. Pressure in the chamber is measured with a Bayard-Alpert-type ion gauge and can be maintained below 4×10^{-6} torr when the contaminant load is small.

2.2 EFFUSION CELL

The outgassing products for contaminating the sample surface are generated using an effusion cell, shown schematically in Fig. 2. The effusion cell has a cylindrical aluminum body 8.9 cm (3.5 in.) long with an internal bore of 4.45 cm (1.75 in.) in diameter. One end is closed, and the other end has a replaceable orifice plate and a shutter to interrupt the contamination flux, if required. The material used to produce the outgassing flux is loaded into the open end of the effusion cell. Three band heating elements clamped around the outside of the cylinder are used to heat the effusion cell to the desired temperature, usually 125°C. A platinum resistance temperature detector (RTD) mounted in the effusion cell housing senses the effusion cell temperature. Output of the RTD feeds a proportional temperature controller, which varies the power applied to the heaters keeping the effusion cell temperature within 1°C of the set point. The controller has an analog output from which the effusion cell temperature is recorded. The effusion cell is capable of maintaining temperatures from ambient to 200°C.

To obtain equal contaminant thickness on the quartz crystal microbalance (QCM) thickness monitor and the sample surface (mirror or solar panel), both surfaces are located equidistant from the effusion cell exit and symmetrically about the effusion cell axis.

The effusion cell is lined with disposable aluminum foil liners. The liners and aluminum foil sample boat are baked out at 125°C for 24 hr prior to each material test. This ensures that the deposited contaminants come from the material being tested and not the peripheral components. New aluminum foil liners and boats are installed after each material test. To terminate the effusion cell output, the effusion cell is equipped with a shutter that can be closed.

2.3 QUARTZ CRYSTAL MICROBALANCE (QCM)

For measuring the mass deposition on a 25°C surface, a water-cooled QCM is used. As stated earlier, the QCM and the sample-collecting surface are located equidistant from the effusion cell exit and symmetrically about the effusion cell axis.

A QCM is based on the principle that the oscillation frequency of a quartz crystal varies proportionally to its mass or any mass adhering to the crystal surface. The oscillation frequency is also dependent upon other things such as temperature. To compensate for temperature effects, the QCMs selected are made up of two quartz crystal oscillators in a single housing (Fig. 3). The oscillator outputs are mixed, and their difference frequency is monitored. One crystal oscillator (the reference oscillator) is enclosed and shielded from contaminants, seeing temperature effects but not contaminants. One surface of the other quartz crystal oscillator is polished to an optical finish and overcoated with aluminum. It is exposed to the contaminant

7

flow and is used as the mass-sensing oscillator. The change between the two oscillator frequencies, (i.e. the change in the difference frequency) is attributed to the accumulated mass from the contaminant.

The relation between the difference frequency change (df) and the deposited mass (dm) can be expressed as (See Ref. 5)

$$dm = 1.4 \times 1.0^{-9} \, df \, (gm \times Hz^{-1}) \tag{1}$$

or

$$\frac{dm}{A} = 4.43 \times 10^{-9} \, df \, (gm \times cm^{-2} \times Hz^{-1}) \tag{2}$$

where A is the surface area of the sensing crystal electrode, 0.316 cm^2. When S is the specific gravity for the condensed film, the change in film thickness (dt) can be calculated from the difference frequency change (df) using the equation

$$dt = 4.43 \times 10^{-9} \, S^{-1} \, df \, (cm \times Hz^{-1}) \tag{3}$$

where dt is given in cm and df is given in Hz. For the results presented, a specific gravity of 1.0 was assumed.

Both quartz crystals have AT crystal cuts selected to minimize temperature effects at the selected operating temperature. In this case, the crystal cut is optimized for 25°C operation by using crystals with an AT cut of 35.2 deg. Temperatures of the QCM and the sample are stabilized by flowing water through passages in the QCM housing and the sample arm.

The QCM has a platinum resistance device (RTD) placed between the sensing and reference crystals, which functions as both a temperature sensor and a low-power (2-W) heater through a time-sharing electronics circuit. In this way, the temperature of the crystals may be monitored and small temperature changes made.

The QCM electronic controller has three analog outputs. They are mass, temperature, and mass rate. In addition, the frequency can be sent to a counter or a frequency-to-voltage converter. The mass deposited on the sensing crystal is determined by recording the change in mass directly or by monitoring the difference frequency between the sensing crystal and the reference crystal.

8

2.4 CONTAMINATION DEPOSITION SURFACES

The sample mirrors consisted of 2.5-cm-diam nickel mirrors with a bare aluminum coating. For reflectance measurements, the front surface of the mirrors needed to be mounted in the same relative position as the front surface of the 1-cm-thick Spectralon® reference sample. To accomplish this, a 1-cm-diam aluminum spacer was Epoxied to the back of the mirror with a low outgassing adhesive. The mirror assembly was then mounted to the positioning arm of the SAM Chamber. The positioning arm was maintained near 25°C by flowing potable water through it.

2.5 REFLECTANCE MEASURING APPARATUS

The reflectance measurement apparatus consists of a Beckman DK2A, double beam, quartz prism, spectrometer with the Beckman integrating sphere reflectance attachment. The reflectance attachment was modified by removing the internal sphere and redirecting the two optical beams into an external integrating sphere attached to the SAM Chamber and maintained at the same pressure as the SAM Chamber. The reflectance sample mirror is mounted to a positioning arm that can be translated and rotated (See Fig. 1). For reflectance measurements, the sample mirror is inserted in the integrating sphere. To contaminate the mirror, the arm is retracted until the mirror is in front of the effusion cell.

The Beckman DK2A consists of a light source housing that directs light into the entrance slit of a quartz prism monochromator. The monochromatic light leaving the monochromator exit slit passes through a 480-Hz chopper to a cam-driven oscillating mirror. The oscillating mirror alternately directs the light into two different optical paths. The light in the first optical path, the sample beam, is directed toward a mirror that focuses an image of the exit slit upon the reflectance sample inside the integrating sphere. The light traversing the second optical path, the reference beam, is directed to a second mirror that projects an image of the slit upon the inside sphere wall. The optical signal is converted to an electrical analog by a light detector viewing the inside of the sphere through a fused silica window. The original Beckman vacuum tube electronics were upgraded by purchasing solid-state electronics (Ref. 6). The solid-state electronics demodulate the sample and reference signals, then output the ratio of sample to reference signal in both analog and digital form. The analog of the ratio of the output is recorded on the Beckman X-Y plotter, and the digital version of the sample-to-reference-signal ratio is recorded by a computer. The Beckman mechanically scans the wavelength range of 250 to 2,300 nm. A 13-bit absolute encoder was added to the prism drive gear to provide a digital output of the wavelength for the computer to record.

Two light sources are used. A deuterium lamp is used for wavelengths less than 350 nm, and a tungsten halogen lamp is switched in place for wavelengths greater than 350 nm. Two

9

light detectors are also used. For wavelengths less than 650 nm, a 1P28B bialkali cathode photomultiplier tube is used; whereas for wavelengths greater then 650 nm, a lead sulphide detector is used.

The reference beam signal is kept at a constant value by adjusting the slit width using the Beckman's slit servo for the lead sulphide detector and servoing the detector high voltage for the photomultiplier tube. The external integrating sphere is 20 cm (8 in.) in diameter with three ports. One port, with a 5-cm diam, was used to attach the integrating sphere to the SAM Chamber for reflectance sample insertion. The second port, with a 3-cm diam and a fused silica window, was used to pass the light into the sphere. The third port, with a 3-cm diam and a fused silica window, was located on top of the sphere out of the plane of the first two ports. The third port was used by the light detectors.

As much as practical, the sphere was configured to meet the requirements set forth by Edwards (Ref. 7) for absolute reflectance measurements as follows:

1. A baffle was placed so that the detector could not see the light impinging on the reflectance sample.

2. No baffle was used between the detector and where the reference beam impinged on the sphere wall.

3. The ratio of the sphere port area to sphere wall area was minimized.

4. A diffuse sphere wall was used.

5. All of the sphere wall was seen by the detector.

The first two requirements were met by locating a baffle between the detector and the reflectance sample. The third, minimizing the port-to-sphere surface area, was the reason for increasing the sphere diameter from 15 cm as originally supplied with the reflectance attachment to 20 cm. The area of the ports on the 20-cm sphere amounted to eight percent of the sphere wall area. The fourth, a diffuse sphere wall was obtained by coating the inside of the sphere with a barium sulfate paint available from Eastman Kodak (Ref. 8). The last requirement was not met since the detectors were mounted outside the vacuum window limiting their field of view. This limited field of view made the integrating sphere sensitive to the angular distribution of the reflected light.

10

2.6 SOLAR LAMP

A 1-kW xenon lamp with a fused silica condenser lens was used for the solar irradiance simulator. Initially, the lamp and fused silica cell window were calibrated at 1 kW against an irradiance standard (Fig. 4). The radiation peak near 0.9 μm was not considered a serious defect for the intended use. The lamp was found to overheat at that level; therefore, it was operated at 650 W with the irradiance determined using a calibrated thermopile and transferring the calibration to a silicon cell mounted outside the chamber for relative intensity changes. The total irradiance measured by the thermopile is reported as total solar equivalent (total suns) irradiance using the air mass zero solar equivalent value of 135 mW $\times$ cm^{-2}.

The solar lamp was controlled by a constant current power supply. This maintained the total irradiance at a constant value. To monitor the ultraviolet portion of the spectrum as the lamp aged, an IP28 photomultiplier tube with a Corning CS7-54 bandpass filter (250 to 400 nm) was mounted outside the chamber. This gave a relative indication of the change in the ultraviolet irradiance as the lamp aged.

An example of the decay in the ultraviolet output as the lamp aged is shown in Fig. 5. This represents a deviation from proper simulation of the ultraviolet portion of the solar spectrum that became worse as the lamp aged. The acceptability of this ultraviolet decay depends upon the main cause of the deterioration of the contaminant films. If the deterioration of the contaminant films is determined by total radiation energy, then the simulation should be acceptable; however, if it is predominantly an ultraviolet effect, the decay of the lamp ultraviolet output makes it difficult to correlate the contaminant film decay with the ultraviolet radiation exposure.

The irradiance distribution of the xenon lamp was measured inside the SAM Chamber. This distribution is presented in Figs. 6 and 7. This was large enough to cover the mirror with a flat distribution. The solar cell mounting assembly was larger than the flat portion; but once the solar cell irradiation was started, the assembly was not moved, eliminating position-dependent output changes.

2.7 DATA ACQUISITION SYSTEM

A microcomputer with a hard disk and a floppy disk storage media was used to acquire and store the data from the measurements. The reflectance data were obtained directly from the spectrometer in digital form. The LUSI® electronics transmitted digital intensity data at the rate of 10 readings/sec. For each intensity reading received, the computer would read the spectrometer wavelength from a 13-bit digital encoder mounted to the spectrometer prism drive gear. This resulted in approximately 5,000 points for each spectrometer scan. These data were recorded on a floppy disk and transferred to another computer for off-line reduction.

11

A 64-channel data logger was used to read the analog voltages from the chamber transducers such as pressures, temperatures, QCM controller output, solar cell output, and the solar lamp intensity monitors. When not being used to read the spectrometer, the microcomputer recorded the selected channels from the data logger at selected intervals varying between 1 min and 4 hr.

3.0 EXPERIMENTAL TEST PROCEDURE

3.1 INTRODUCTION

As presented earlier, the primary goal of this work was to study the absorptance change with contaminant thickness and obtain absorptance change with solar irradiation time. Three materials were investigated: a silicone, Dow Corning 93-500 encapsulant; an organic material, Furane Products Uralane 5753-A/B(LV); and an Epoxy laminate, Polyclad FR-4. An additional goal was to investigate the effect of a solarized contaminant film on a solar cell.

The contaminating samples were prepared, installed in the SAM Chamber, and heated to 125°C; the contaminants were then condensed on the 20 to 25°C aluminized mirror (or solar panel). The degradation with contaminant only was measured; then the mirror (or solar panel) was turned toward the solar lamp and irradiated at approximately 0.75 total suns while being cooled by 20 to 25°C potable (tap) water. The degradation was periodically measured and recorded.

3.2 SAMPLE PREPARATION

The two component samples were prepared as specified by the manufacturer and weighed to the specified mixing ratios. One component was added to a disposable aluminum mixing container and weighed; then the other component was added until the correct mixing ratio by weight was obtained. Weighings were made on an analytical balance capable of 0.1-mg precision. After preparation, the sample material was transferred to a previously outgassed and weighed aluminum foil boat. The boat had nominal dimensions 4 × 2.5 × 2.0 cm deep, weighed to 1 gm, and filled with 10 gm of sample material. The material sample was cured and put in a 50-percent relative humidity container for at least 24 hr.

The cure used varied with the material. The DC93-500 encapsulant samples were cured at room temperature and conditioned for nominally 1 week. The manufacturer's cure schedule of 8 hr at 95°C, plus 24 hr at 25°C, was used with the Uralane sample. The Epoxy laminate, FR-4, was taken as received, sliced into 1-cm squares to expose virgin material, and put into the 50-percent relative humidity container.

3.3 EFFUSION CELL PREPARATION

Prior to the first test of each type of material, the effusion cell interior was cleaned with Freon, and a new foil liner was installed. The effusion cell was then outgassed under vacuum at 125°C for 24 hr.

3.4 QCM PREPARATION

The QCM was cleaned with ethyl alcohol or Freon and dried under vacuum. The QCM was mounted at a symmetric location at the same distance horizontally from the effusion cell aperture and vertically from the effusion cell centerline as the test surface (mirror or solar cell).

3.5 MIRROR PREPARATION

The aluminum overcoated nickel mirrors were provided by WRDC. Prior to installation in the chamber, a cylindrical aluminum (1-cm-long by 1-cm-diam) mounting adapter was bonded to the rear surface of the mirror. A low outgassing Epoxy bonding adhesive was used. The assembly was cured at 60°C for 12 or more hours prior to installation in the SAM Chamber. The pretest reflectance scans of the mirror were taken under vacuum to minimize changes in the optical path by shifting of the integrating sphere windows with sphere pressure change.

3.6 RELATIVE REFLECTANCE MEASUREMENT

The reflectance degradation test proceeded as follows:

1. The QCM was located with respect to the mirror and the effusion cell, and cooling water to the QCM and the mirror sample arm was turned on. The cooling water to the sample arm and the QCM were series-connected to provide similar cooling water conditions.

2. The Spectralon® reference sample was mounted on the sample arm and scanned with the spectrometer for a reference measurement; then the clean sample mirror was mounted.

3. The material sample was installed in the effusion cell, and the effusion cell shutter was closed.

4. The SAM Chamber was closed and pumped down.

5. Under vacuum, the sample mirror was inserted into the integrating sphere for a reflectance measurement. Because the mirror was a specular reflector, care was taken to rotate the mirror to a precise index point after it was inserted. This minimized the potential effects of the integrating sphere, angular distribution sensitivity.

6. The sample mirror was retracted to face the effusion cell.

7. The effusion cell shutter was opened, and the effusion cell temperature was increased to 125°C.

8. The contaminant buildup was monitored by observing the QCM frequency change. Near the desired thickness, the mirror was reinserted into the integrating sphere; a reflectance measurement was made; the mirror was retracted; and the contamination of the mirror was resumed.

9. Repeat spectral measurements were made as desired.

10. When the desired contaminant level was obtained, the effusion cell was closed and the heaters turned off. Then a final reflectance measurement was made, and the solar degradation was started. The mirror was located facing the xenon solar lamp for solar irradiation. The xenon lamp current was set to 18.0 amp for the DC93-500 and 30 amp for the other materials. This corresponded, respectively, to total irradiances of 0.4 and 0.75 total suns at the sample.

11. At the desired times, the mirror sample was inserted in the integrating sphere to measure the degraded reflectance, then retracted for continued solar irradiation.

3.7 ABSORPTANCE CALCULATION

The absorptance (alpha) obtained is the integral of the spectral absorptance weighted by the standard solar irradiance spectrum at one astronomical unit distance, air mass zero (Ref. 9). The results reported are the differences between the baseline, the integrated absorptance of the uncontaminated mirror, and the contaminated mirror integrated absorptance (delta alpha).

The relative spectral absorptance is taken to be one minus the spectral reflectance. The integrated solar absorptance can be represented as follows:

$$\alpha = 1 - \frac{\int RE \, d\lambda}{\int E \, d\lambda} \qquad (4)$$

where

α = the integrated, solar-weighted, relative absorptance; unitless

R = the relative spectral reflectance of the mirror; unitless

E = the standard solar spectral irradiance outside the earth's atmosphere; $W \, cm^{-2} \, \mu m^{-1}$

λ = spectral wavelength; μm

The limits of integration are defined to be over the entire solar spectrum; however, the range 0.25 to 2.3 μm contains 95 percent of the solar irradiance. This spectral range was used for the absorptance determination.

The computer program that calculated the absorptance proceeded as follows:

1. The standard spectral irradiance values, E, for air mass zero were stored in a table.

2. The spectral reflectance measurements, R, for the 0.25- to 2.3-μm region were read into a table.

3. The R and E data were interpolated to obtain 500 values from 0.25 to 2.3 μm.

4. The absorptance was calculated using

$$\alpha = 1 - Sum \, (R_i \, E_i)/Sum \, (E_i)$$

where the sums are over all 500 points.

5. The change in absorptance was taken as the difference between the clean mirror absorptance and the contaminated mirror absorptance.

3.8 SOLAR CELL DEGRADATION TEST

A solar cell mounting plate was constructed from an 80- by 100- by 6-mm-thick piece of aluminum. For ease of handling, each of three solar cells and solder tabs for lead wires

were bonded to 60- by 20- by 2-mm-thick strips of aluminum using Dow Corning 93-500 encapsulant. These aluminum strips were mounted to the aluminum plate with screws. The 2- by 2-cm solar cells were mounted to the plate so that all three were at the same radial distance from the effusion cell centerline as the QCM. Mounted near the center of the aluminum plate was a calibrated thermopile used for initial setup of the solar lamp. The panel was cooled by a water-cooled copper plate attached to the backside of the aluminum plate with screws. The panel temperature was monitored by a platinum resistance temperature sensor bonded to the panel backside.

The solar cells were wired so that by changing a switch position, their output was (1) open circuit (no current could flow), (2) into a total load that was optimized for maximum power at 25°C, or (3) into a 1-ohm resistor to simulate a short circuit. The output current was read by reading the voltage drop across the 1-ohm resistor that was in the circuit for the maximum power and the short-circuit cases. The output voltage was read across the pins of the chamber electrical feedthrough. For each solar cell, the output voltage and currents were recorded on the data logger.

A calibrated thermopile was mounted near the center of the solar cell mounting plate. It was used in initial tests to determine the irradiance level for different lamp currents and to calibrate the silicon detector mounted outside the SAM Chamber. The outside silicon detector was used to monitor the xenon lamp output during the solar runs.

The solar cell test procedure was as follows:

1. The QCM was aligned with the solar panel similar to the mirror degradation test.

2. The contaminant sample was removed from the 50-percent relative humidity container, weighed, and installed in the effusion cell as described previously.

3. The SAM Chamber was pumped down, and the cooling water was turned on. The cooling water passed in series through the QCM and solar panel to keep them near the same temperature.

4. The solar panel was turned toward the solar lamp, and the lamp was adjusted to the desired current level. Data logger recordings were taken of the solar cells and the radiation detectors with the load switches in the short-circuit, open-circuit, and maximum power positions.

5. Contamination was initiated by turning the solar panel toward the effusion cell, opening the effusion cell flapper, and bringing the effusion cell temperature to 125°C.

6. The QCM was monitored to determine the contamination accumulation. At the desired contamination level, the effusion cell shutter was closed, the effusion cell heater turned off, and the solar panel turned toward the xenon solar lamp for the solar degradation portion of the test.

7. The solar degradation was started by setting the lamp current, taking readings in the three load switch positions, and then recording the solar cell short-circuit current output with time. Periodically, solar cell output was recorded for the three load switch positions.

4.0 RESULTS AND DISCUSSION

4.1 MIRROR CONTAMINATION RESULTS

4.1.1 Dow Corning 93-500 Space-Grade Encapsulant

The mirrors were exposed to DC93-500 contaminant from the effusion cell until the desired contaminant thickness was obtained. The contaminated mirrors were then exposed to 0.4 total suns irradiance levels from the xenon lamp. An example of the raw relative reflectance variation with contamination thickness is shown in Fig. 8. It can be seen that for 900 Å contaminant thickness, there was a 2- to 8-percent change in the ultraviolet and visible portions of the spectrum. Changes in the spectrum above 1,200 nm are attributed to instrument repeatability effects. A small step occurs at 650 nm where the detectors were switched. This is attributed to the change in detector to sphere wall view factor that occurs when the detectors are switched. The ideal detector-mounting position is on the sphere wall allowing full view of the sphere inside surface; however, the limitations imposed by the vacuum seal on the detector viewing port restrict the detector view. This restriction is greatest for the photomultiplier tube; hence, the photomultiplier has the larger deviation from ideal sphere performance.

The sensitivity of the integrating sphere to the angular distribution of light invalidated the use of a diffuse reflector of known reflectance to calibrate the reflectance of a specular mirror, as originally intended. However, as long as the angular distribution of the light reflected from the sample mirror does not change appreciably, and the mirror is carefully positioned to the same angle in the sphere, changes in the reflectance are still valid. This approach, looking at the reflectance change, was used to measure the mirror degradation.

An example of the QCM-measured contaminant thickness variation with time is presented in Fig. 9. The rate of the initial thickness buildup is influenced by the time it takes for the effusion cell to reach 125°C, usually about 0.5 hr.

17

The effect of the 0.4 total suns solar irradiation on the DC93-500 contaminant is shown in Figs. 10 and 11. During the solar irradiation, the measured temperature of the mirror-mounting arm typically varied between 24 and 28°C. It is assumed that the 1-cm-diam aluminum mirror mounting slug kept the mirror surface near this temperature.

In Fig. 10, the shift in the reflectance spectra beyond 1,200 nm is attributed to an instrument shift of unknown cause. The reflectance spectra between 400 and 600 nm had an increase in reflectance with solar irradiation before continuing the degradation. Possible causes of this effect, such as evaporation of the contaminant film with irradiation, requires further investigation. One method to evaluate possible evaporation is to irradiate the contaminated QCM while the mirror is being irradiated. This would detect changes in the film thickness; however, irradiating the contaminant on the QCM makes the contaminant difficult, if not impossible, to remove. This permanent film would limit further usefulness of the QCM.

The xenon solar lamp had considerable degradation of its ultraviolet output as is shown by the ultraviolet radiation monitor (Fig. 5). During the first 400 hr of operation, the ultraviolet output, in the 250- to 400-nm band, deteriorated to 35 percent of its initial value. The rate of degradation seemed to decrease as the lamp aged.

The change in integrated solar absorptance calculated from the measured reflectances are shown versus thickness (Fig. 12) and versus irradiation time (Fig. 13). The degradation results in Fig. 13 are presented on the basis of constant total irradiance on the sample. This assumes that the degradation of the contaminant film is related to the total solar irradiance. However, if the degradation is primarily from the ultraviolet portion of the spectrum, the results can be misleading. This is because the ultraviolet output of the lamp at a constant total irradiance is continually dropping as the lamp ages, showing less degradation than would be seen for irradiation at constant ultraviolet output.

The Run 7 solar degradation rate slowed at 30 hr, and this was attributed to pressure-dependent effects. The pressure rise occurred when the chamber was valved off from the pumps when the turbomolecular pump started to fail. With no pumping, the chamber gradually leaked to a pressure of 7 torr when the test was terminated at 280 hr. This pressure dependence could come from the increased presence of oxygen in the SAM Chamber. The ultraviolet light could convert oxygen to ozone, which in turn could interact with the contaminant film.

4.1.2 Furane Products Uralane 5753-A/B(LV)

Two mirrors were tested with Uralane contaminant thicknesses of 110 and 280 Å. After contamination, the mirrors were illuminated with the xenon lamp at an irradiance of 0.75 total suns.

The effect of the contaminant prior to irradiation was, at these thicknesses, less than the instrument noise beyond 600 nm and showed small, 2- to 3-percent, changes at wavelengths shorter than 600 nm (Fig. 14). An example of the contaminant deposition measured by the QCM is shown for the first Uralane sample (Fig. 15). The second Uralane-contaminated mirror, not shown, had contaminant deposited in two segments. A deposit thickness was obtained, and the effusion cell was closed with heat turned off for the weekend. The two days under vacuum resulted in a major portion of the contaminant evaporating from the QCM, and it was assumed that the contaminant also evaporated from the mirror. To achieve the desired contaminant thickness, a second contaminant layer was deposited on the remnants of the first layer. The solar degradation of the second mirror is shown in Figs. 16 and 17. The short wavelength end of the reflectance spectrum showed considerable degradation with the reflectance at 255 nm decreasing to 16 percent of the original reflectance. The changes between 1,400 and 2,200 nm are less than the instrument repeatability.

Inspection of the second Uralane sample after removal from the effusion cell showed that the sample had not completely solidified. A third sample was mixed and cured to check the resin and hardener components. This third sample cured solid, but was sticky around the edges. This implies that the second sample was improperly mixed.

The integrated solar absorptance, alpha, is shown for contamination thickness in Fig. 18 and the solar irradiation time in Fig 19. In both cases, the change in alpha is referenced to the uncontaminated mirror. It can be seen that the 110 Å layer from the second Uralane sample degraded faster than the 280 Å layer from the first sample. This is attributed to the improper hardening of the second sample leaving a different mix of contaminant products on the mirror. The results of this second sample are presented to show the degradation trend with the extended solar irradiation time (1,265 hr).

4.1.3 Polyclad FR-4 Epoxy Laminate

Because of suspected contamination from the preceding Uralane test, the effusion cell was cleaned and a clean mirror was irradiated at 0.75 total sun level for 230 hr with no contaminant source in the effusion cell. This clean mirror test was used as a tare run. A spectral reflectance scan of the tare mirror following irradiation showed reflectance degradation in the violet end of the spectrum (250 to 500 nm). The worst tare mirror reflectance degradation was 0.3 at 255 nm.

Three more tare mirrors were tested before the FR-4 sample was run. Comparison between the last tare mirror degradation and the FR-4 mirror degradation at 255 nm is shown in Fig. 20. The rate of the contaminant reduction, judged from the tare runs, implies that the introduction of the contaminant into the chamber occurred relatively recently. It was felt

that the chamber contamination occurred when the second, unhardened, Uralane sample was tested just prior to the FR-4 test.

The FR-4 sample mirror was coated with an 80 Å layer of contaminant from the FR-4 material and then illuminated with the xenon lamp at an irradiance level of 0.75 total suns. The raw reflectance variation is shown in Figs. 21 and 22, and the change in integrated solar absorptance in Fig. 23. The corrected curve was obtained by subtracting the smoothed tare curve from the corresponding values for FR-4.

4.2 SOLAR CELL RESULTS

Three solar cells, one silicon and two gallium arsenide, were attached to an instrumented, water-cooled, mounting plate. The solar cells were contaminated with DC93-500 outgassing products to a contaminant thickness, measured by the QCM, of 940 Å. Following contamination, the solar cells were illuminated by the xenon lamp for 614 hr.

The solar cells experienced different levels of irradiance attributable to the extent of the solar cells on the plate (7.5 cm horizontal by 2.5 cm vertical) compared with the size of the xenon lamp beam, which was flat over 6 cm horizontally by 2.5 cm vertically (Figs. 6 and 7). Solar cell S1, a silicon cell, had 1.07 total sun irradiance. Solar cell S2, a gallium arsenide cell, had 0.46 total sun irradiance; and solar cell S3, also a gallium arsenide cell, had 0.49 total sun irradiance. The total sun output of the lamp remained constant over the duration of the test as can be seen by the silicon detector mounted outside the chamber (Fig. 24). The lamp output at the end of the 614-hr period was within 2 percent of the output at the beginning. A thermopile attached to the solar cell mounting plate inside the chamber was within five percent of its reading at the beginning of the test. The ultraviolet output of the lamp continued to degrade as the lamp aged. Spikes in the ultraviolet detector output could be from humidity effects, changing the fraction of the ultraviolet light reaching the detector.

The solar cell mounting plate temperature was monitored and found to stay in the 50 to 53°C range (Fig. 25), higher than the goal of 25°C. This higher temperature had not been encountered on earlier checkout runs with higher irradiance levels. The higher temperature may be caused by reduced heat transfer from deposits that occurred in the water cooling lines.

For a constant irradiance, solar cell output power into a fixed load resistor is very temperature-sensitive. The output voltage varies strongly with temperature (Ref. 10) resulting in a change in the value of the load resistor needed for maximum power transfer. In contrast, the short-circuit output current is relatively insensitive to solar cell temperature changes. For this reason, the short-circuit current was measured instead of the solar cell output power.

The degradation of two of the solar cells is apparent (Figs. 26 and 27). The silicon cell, S1, had a 12-percent drop in the short-circuit current, and the gallium arsenide cell, S3, had a 9-percent drop in the short-circuit current. Not knowing the spectral responses of the two types of solar cells, it is difficult to tell if this degradation difference related to the reduced short-wavelength transmission of the DC93-500 contaminant. However, one possible explanation for the difference could be attributable to the different radiant energy the two solar cells received. The gallium arsenide solar cell received 0.5 total suns irradiance for 614 hr. Using Fig. 13, for the DC93-500 contaminant, this irradiation gives a change in alpha of 0.10. This agrees with the 9-percent drop in the gallium arsenide solar cell output. The silicon solar cell was exposed to 1.1 total suns irradiance for 614 hr. This is roughly twice the irradiance level of Fig. 13. Looking at the effect of double the exposure time, 1,228 hr, gives a change in alpha of 0.13, which agrees with the observed 12-percent drop in the silicon solar cell output. The second gallium arsenide cell, S2, showed degradation trends, but near 160 and 425 hr, it had jumps in output. The cause of these jumps was uncertain; however, after testing, an inspection of the cell leads revealed a broken solder joint that may have contributed to the erratic performance.

4.3 ERRORS

4.3.1 Sample Mixing

The mixture ratios of the two component samples were determined on a mass basis with the mixing container mass being measured after each component was added. The ability to match the manufacturer's specified mixing ratio was not limited by the actual mass measurement, but by the ability to introduce the second component in controlled quantities. The DC93-500 samples were prepared within 6 percent of the manufacturers specified 10:1 ratio (resin-to-hardener) and in most cases within 3 percent of the specified ratio. The Uralane 5753-AB (LV) samples had a 1:5 (resin-to-hardener) mixture ratio. The first Uralane sample was low on hardener by 15 percent. The second sample may have had a mixing error since it never completely solidified.

4.3.2 Contaminant Layer Thickness

The contaminant layer thicknesses were inferred from the frequency change of a QCM placed in a corresponding symmetrical position with respect to the axis of the effusion cell orifice. A detailed analysis of QCM errors is presented in Ref. 11, which reported a bias error of ± 20 percent and precision error ± 26 percent, for a total uncertainty of ± 46 percent. Specific comments with regard to this application follow.

Electrical noise influenced the QCM frequency measurement by less than 5 Hz and had negligible effect on the precision of the thickness measurement. The QCM frequency was observed as the effusion cell temperature was cycled several times between ambient and 125°C, and the QCM frequency was observed during the daily excursions of the SAM Chamber ambient temperature and the QCM cooling water temperature. The combined effects from these sources is estimated to be less than 20 Hz. This amounts to a 10-percent precision error for contaminant films when trying to measure a 200-Hz change (90 Å thickness).

Conversion of the QCM frequency change into contaminant thickness [Eq. (3)] assumes a contaminant specific gravity of 1.0. The specific gravity of the two components of the Uralane 5753-A/B(LV) was 1.0, whereas the specific gravity of the Dow Corning 93-500 components was unknown. Some contaminants such as another form of Uralane (5753-A) have a specific gravity of 1.2, implying a thickness bias error of 20 percent. The contaminant film from Dow Corning 93-500 was observed to be deposited unevenly on the mirror and QCM with spots that looked like a spatter process rather than a gradual, even coating. The magnitude of the error from this effect is unknown.

Positioning of the QCM in a symmetrical position with respect to the axis of the effusion cell orifice is estimated to be within 2 mm of the symmetry point. The nominal geometry of the system was QCM crystal face 2.5-cm horizontal distance from the effusion cell orifice plane, and crystal center 2.5-cm vertical from the axis of the effusion cell orifice. Calculations indicate that a 2-mm error in the vertical position of the QCM corresponds to a 11-percent bias error in the contaminant thickness on the mirror. The overall uncertainty of ±46 percent presented in Ref. 11 appears reasonable for the present case.

4.3.3 Reflectance and Alpha

The reflectance measured was not absolute reflectance; however, changes in the measured reflectance from the clean mirror values effectively removes the repeatable instrument factors and gives the degradation of the mirror from the contaminants.

The precision of the reflectance measurement was evaluated by making 10 reflectance measurement cycles over a period of 240 hr. The reflectance measurement cycle consisted of inserting the mirror in the integrating sphere, making a reflectance scan, then retracting the mirror arm into the solar irradiation position. For a given wavelength, these reflectance measurements had a standard deviation of 0.005 (roughly 0.5 percent of the clean mirror reflectance). However, on other occasions, the instrument was observed to have a 0.01 to 0.03 shift in the reflectance over a portion of the spectrum, usually on the infrared end. In most cases, the cause was obvious and was corrected; but in a few cases, no immediate reason could be found leading to this higher error. The estimated upper limit on the precision of the reflectance is 0.03 (roughly 3 percent of the clean mirror reflectance).

22

Alpha is derived from the reflectance measurements [Eq. (4)]. Because the reflectance is weighted by the solar energy spectrum and is integrated over the solar band, errors at the extremes of the spectrum have little effect, and the random noise in a reflectance scan tends to cancel itself. Looking at the scatter in alpha for repeated reflectance scans, the precision for alpha is estimated to be ±0.01. From measurements of the tare mirrors, it is estimated that the maximum bias error in alpha from background contamination is 0.01 for the measurements presented.

5.0 CONCLUDING REMARKS

Experiments have been performed under vacuum to measure degradation of aluminum-coated mirrors and solar cells by condensed outgassing contaminants followed by solar irradiation.

Results were obtained for the degradation of aluminum mirrors from the following sources:

1. **Dow Corning 93-500 Encapsulant.** The change in integrated solar absorptance (delta alpha) with solar irradiation time is presented for 900 Å contaminant thickness, and an abbreviated delta alpha with irradiation time is presented for 1,500 and 1,600 Å contaminant thicknesses.

2. **Furane Products, Uralane 5753-AB (LV) Encapsulant.** Delta alpha versus solar irradiation time for 110 Å contaminant thickness and an abbreviated delta alpha versus solar exposure for 280 Å thickness is presented. The 110 Å contaminant thickness came from unhardened Uralane sample resulting in different outgassing characteristics from a properly set up sample.

3. **Polyclad FR-4 Epoxy Laminate.** Delta alpha with solar irradiation time is presented for 80 Å contaminant thickness.

Results were obtained for the degradation of silicon and gallium arsenide solar cells with 940 Å thickness of condensed contaminant from Dow Corning 93-500 encapsulant, followed by 614-hr irradiation from a xenon lamp. The degradation of the solar cell output could be explained by changes in the integrated solar absorptance of the contaminant layer using the mirror delta alpha results.

Using the experience gained from these measurements, the following recommendations can be made:

1. To quantify the ultraviolet output of the solar lamp as the lamp ages, spectral irradiance calibrations should be performed between sample runs. The ultraviolet monitor could then be used to interpolate the lamp irradiance between calibrations. In addition, the optical path of the ultraviolet monitor could be purged to reduce chances of outside influences upon the monitor signal.

2. If the degradation of the contaminant surfaces is predominantly an ultraviolet effect, then a source with better ultraviolet emission should be considered. For example, a mercury lamp with its main radiation at 254 nm should be considered, or a mercury xenon lamp with a higher ultraviolet output than a xenon lamp could be considered. Using one of these lamps with frequent calibration, it should be relatively easy to irradiate with constant ultraviolet irradiance.

3. To evaluate possible evaporation effects on the contaminant film reflectance for a material such as Dow Corning 93-500, a constant-temperature water supply could be installed to hold both the sample mirror and the QCM at 25°C. Then, both the sample mirror and the QCM could be irradiated to see if there is a correlation between the reflectance change and a change in the contaminant film thickness.

4. The solar cell response curves can be measured. This, with the measured spectral output of the solar lamp and the spectral degradation of the contaminant films, allows calculation of the solar cell output current for comparison with the measured solar cell output current.

5. An improved detector mount on the integrating sphere is needed to remove the sensitivity of the reflectance measurements to angular distribution of the reflected light.

REFERENCES

1. Storer, Roberta A., Editor, ASTM Designation: E 595—84. "Standard Test Method for Total Mass Loss and Collected Volatile Condensable Materials from Outgassing in a Vacuum Environment." 1988 Annual Book of ASTM Standards, Section 15, Vol. 15.03, ASTM Headquarters, Philadelphia, Pennsylvania, 1988.

2. Glassford, A. P. M. and Garrett, J. W. "Characterization of Contamination Generation Characteristics of Satellite Materials Phase II — Test Method Development." AFWAL-TR-85-4118, December 1985.

3. Wood, B. E. et al. "Surface Effects of Satellite Outgassing Products." *AIAA Journal of Thermophysics and Heat Transfer*, Vol. 2, No. 4, October 1988, pp. 289-295.

4. Hall, D. F., Stewart, T. B., and Hayes, R. R. "Photo-Enhanced Spacecraft Contamination Deposition." AIAA Paper 85-0953, Presented at the AIAA 20th Thermophysics Conference, June 19-21, 1985.

5. Operation and Service Manual for Quartz Crystal Microbalance, QCM Sensor Mark 9, QCM Research, Laguna Beach, California.

6. LUSI III Manual, Lehr, Inc. *dba Spectra Instrumentation*. Auburn, California.

7. Edwards, D. K. et al. "Integrating Sphere for Imperfectly Diffuse Samples." *Applied Optics*, Vol. 51, November 1961, pp. 1279-88.

8. Grum, F. and Luckey, G. W. "Optical Sphere Paint and a Working Standard of Reflectance." *Applied Optics*, Vol. 7, November 1968, pp. 2289-94.

9. Rauschenbach, H. S. *Solar Cell Array Design Handbook*. Van Nostrand Reinhold Company, New York, 1980 (First Edition).

10. Green, Martin A. *Solar Cells, Operating Principles, Technology, and System Applications*. Prentice-Hall, Inc., Englewood Cliffs, N.J., 1982 (First Edition).

11. Alt, R. E. "Bipropellant Engine Plume Contamination Program, Volume I Chamber Measurements — Phase I." AEDC-TR-79-28 (AD-A077435), December 1979.
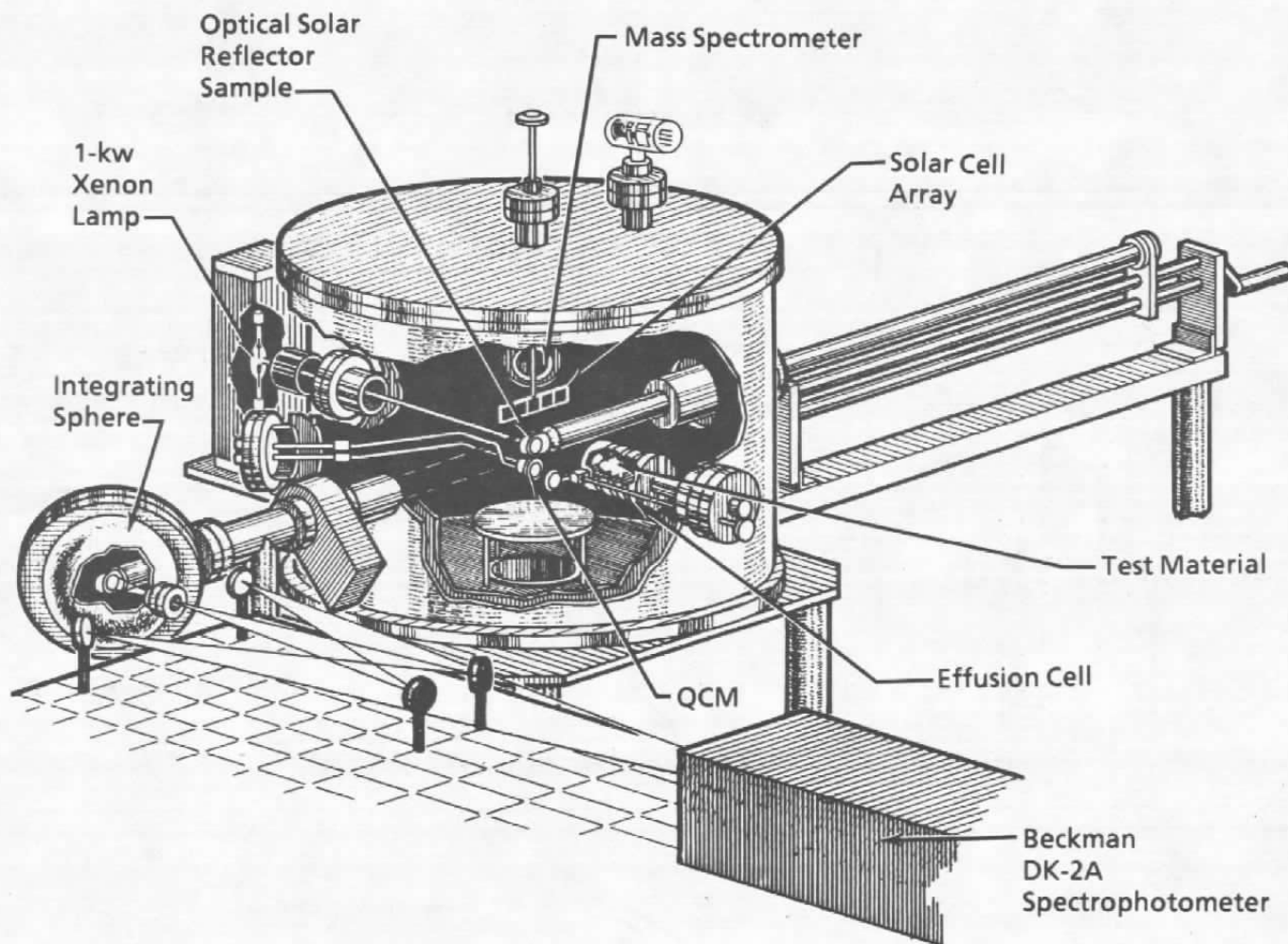
Figure 1. Solar Absorptance Measurements Chamber.

Optical Solar Reflector Sample

Mass Spectrometer

1-kw Xenon Lamp

Solar Cell Array

Integrating Sphere

Test Material

Effusion Cell

QCM

Beckman DK-2A Spectrophotometer

Figure 2. Effusion cell.

Cover

Plug-In Crystal
Heater Assembly

Connector Assembly

Oscillator/Mixer
Hybrid Circuit
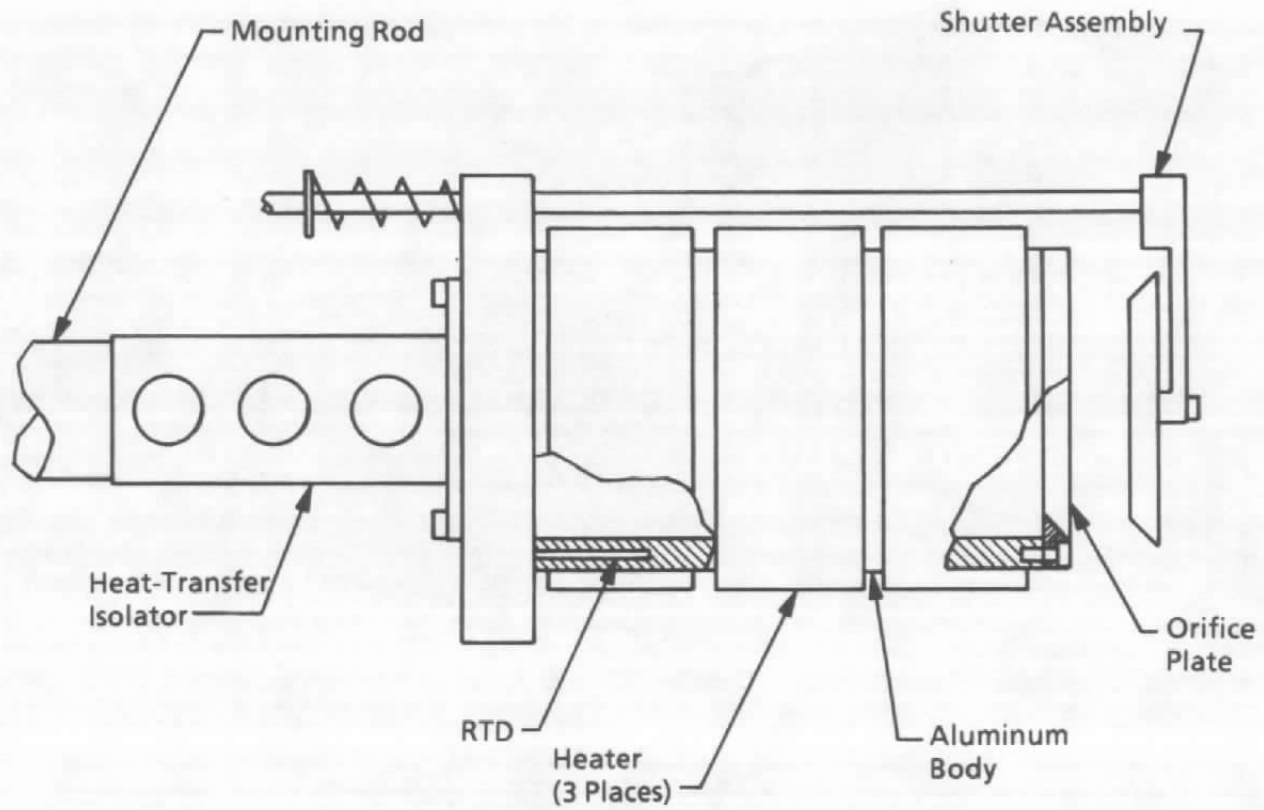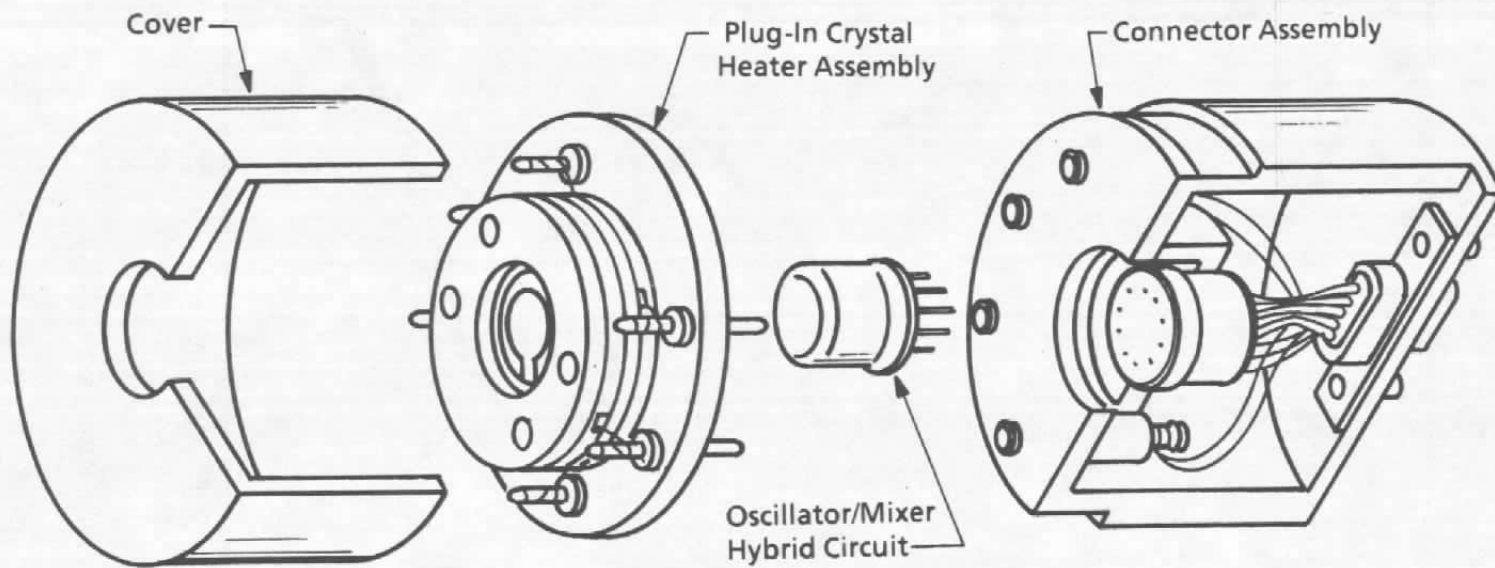
Figure 3. Quartz crystal microbalance, exploded view.
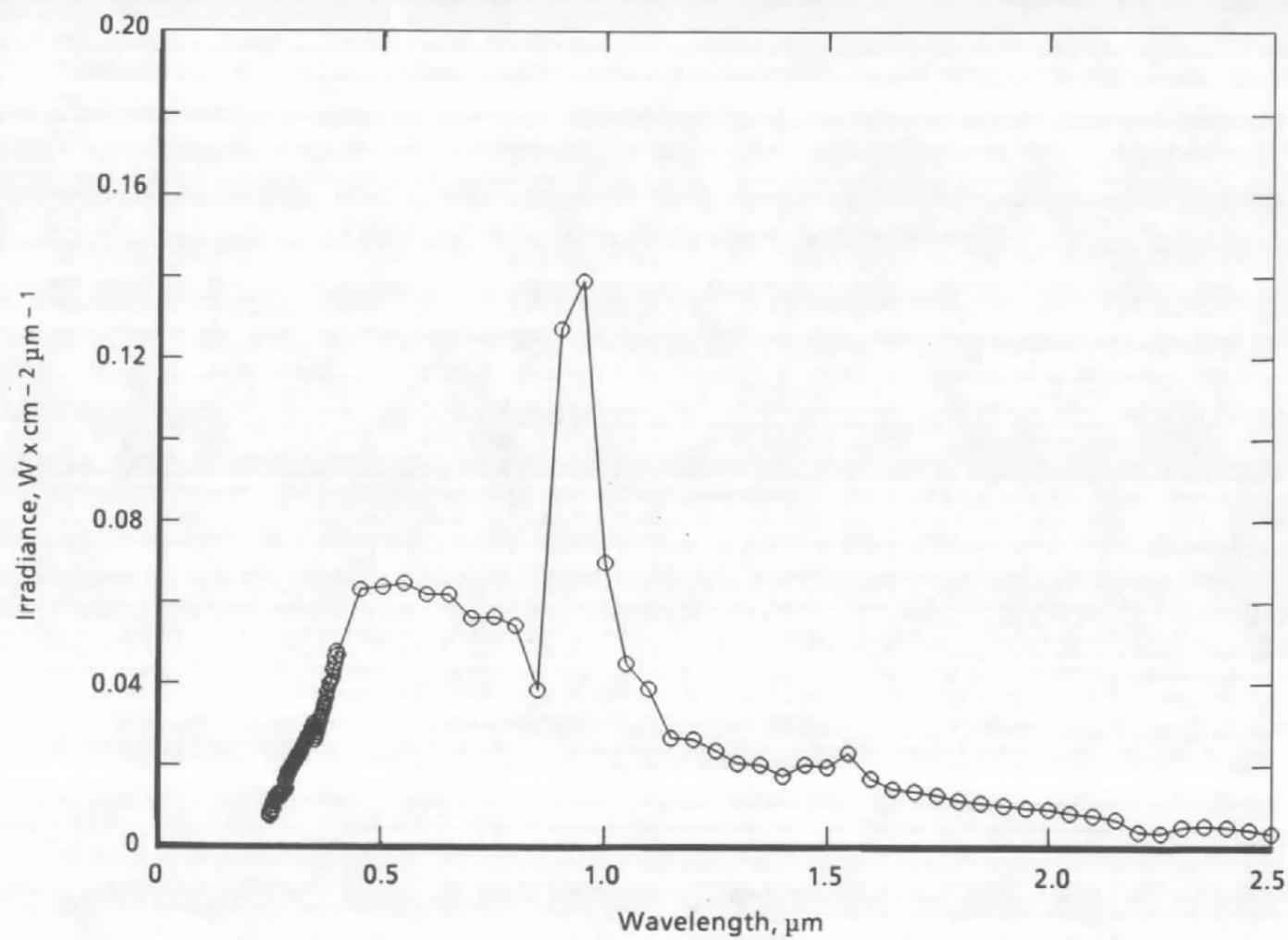
Figure 4. Spectral irradiance of xenon solar lamp at 50 cm.
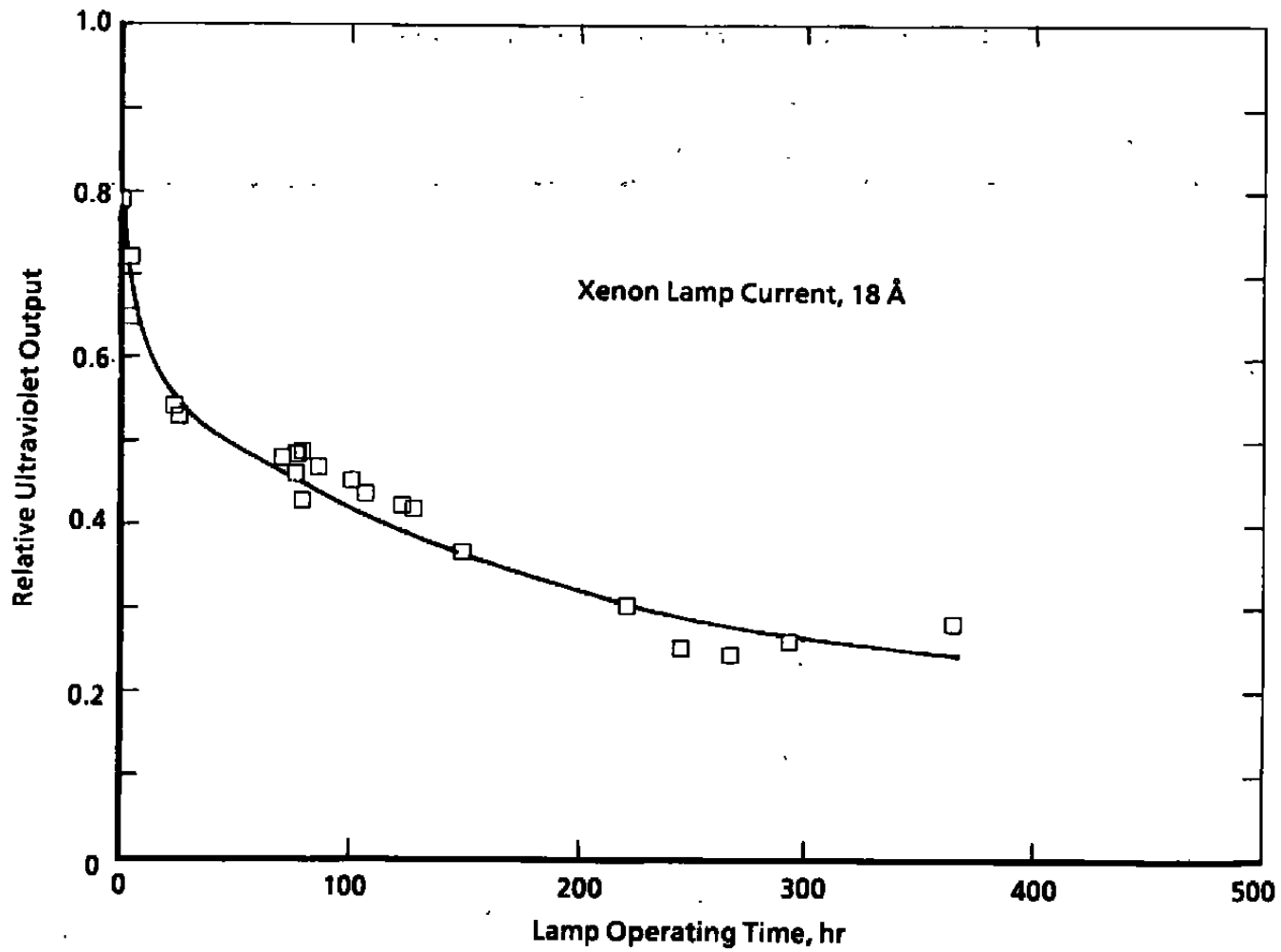
Figure 5. Decrease in lamp ultraviolet output with time.
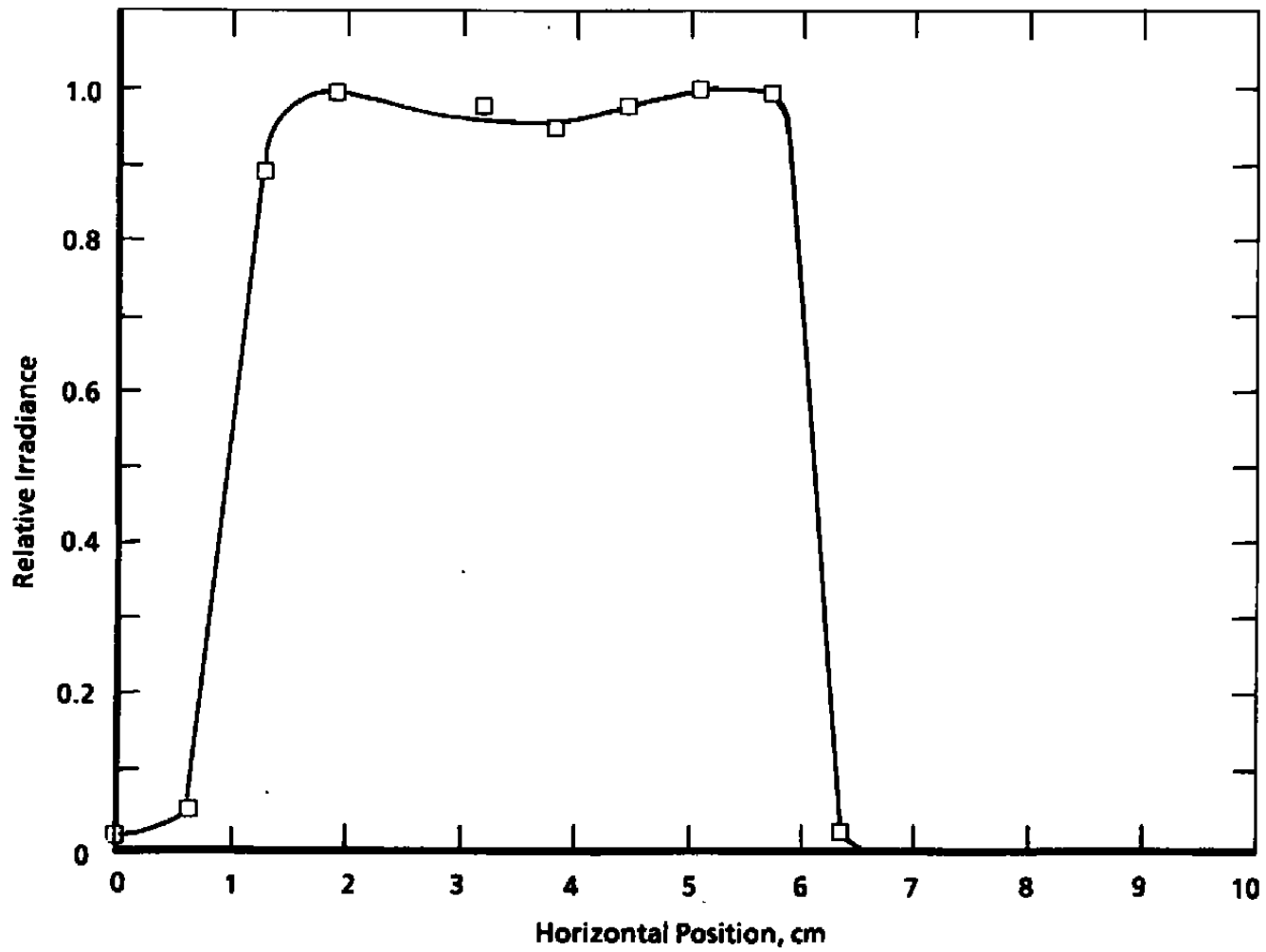
Figure 6. Horizontal distribution of lamp irradiance at 50 cm.
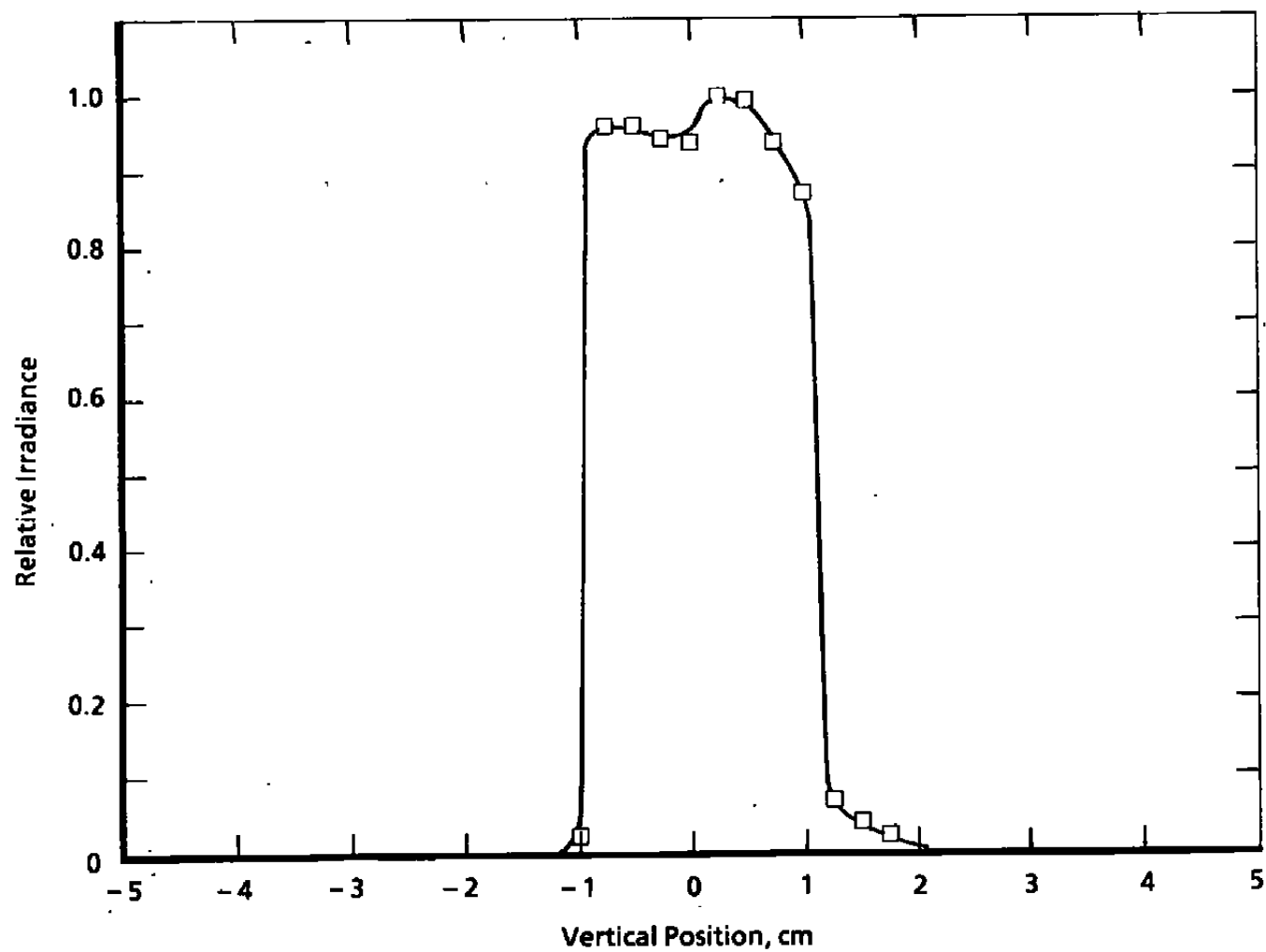
Figure 7. Vertical distribution of lamp irradiance at 50 cm.
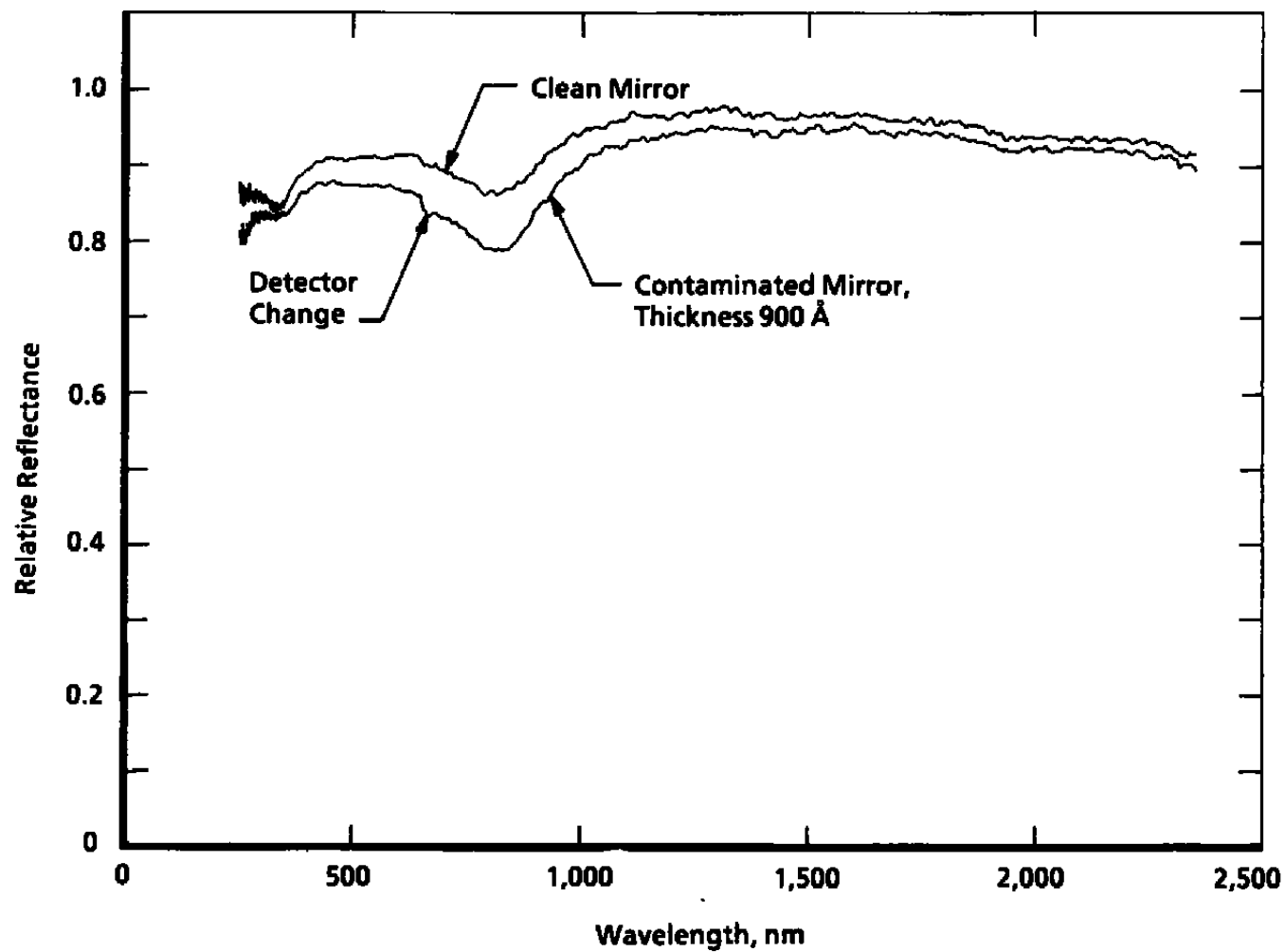
Figure 8. Effect of contaminant upon mirror reflectance, DC 93-500.
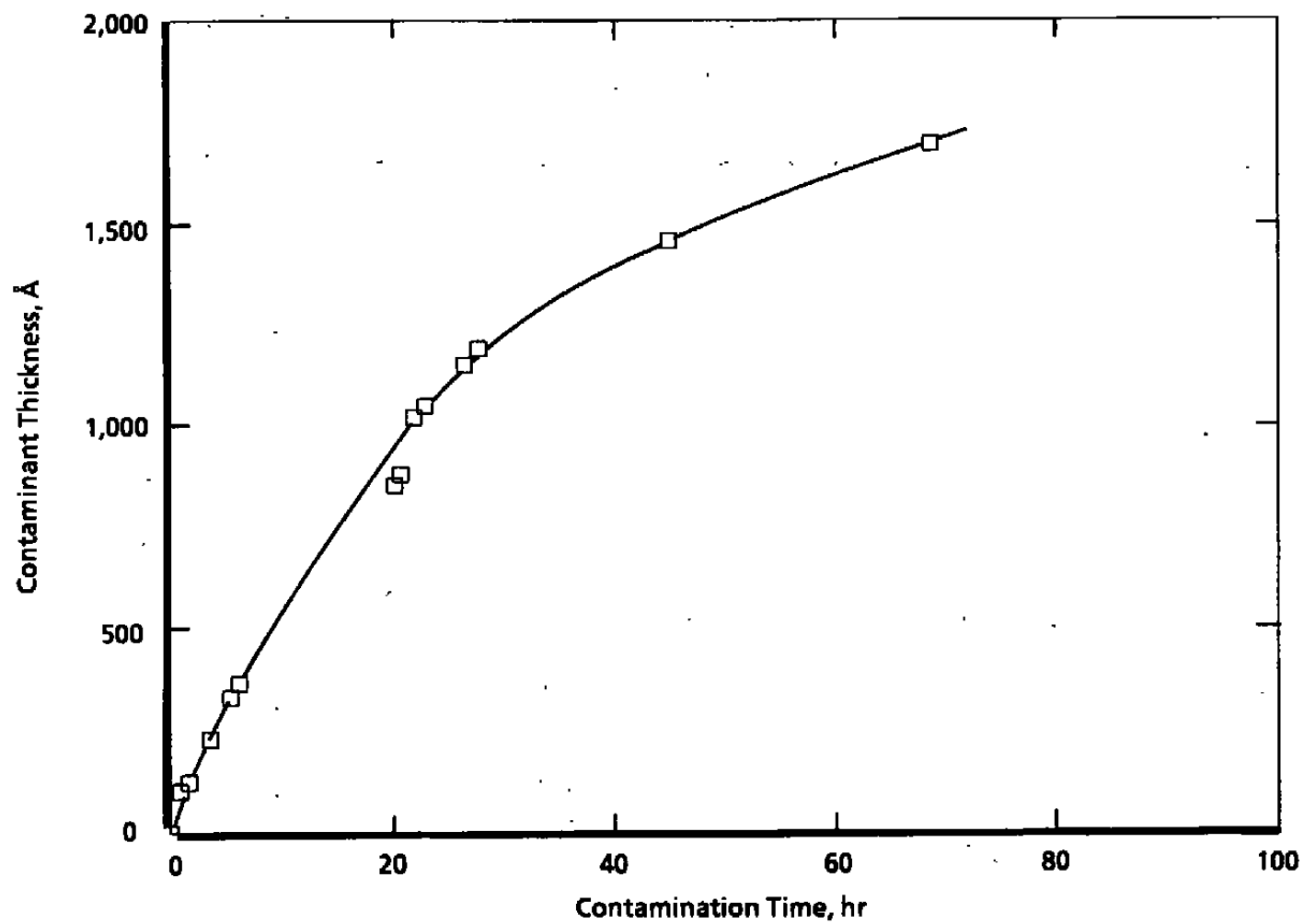
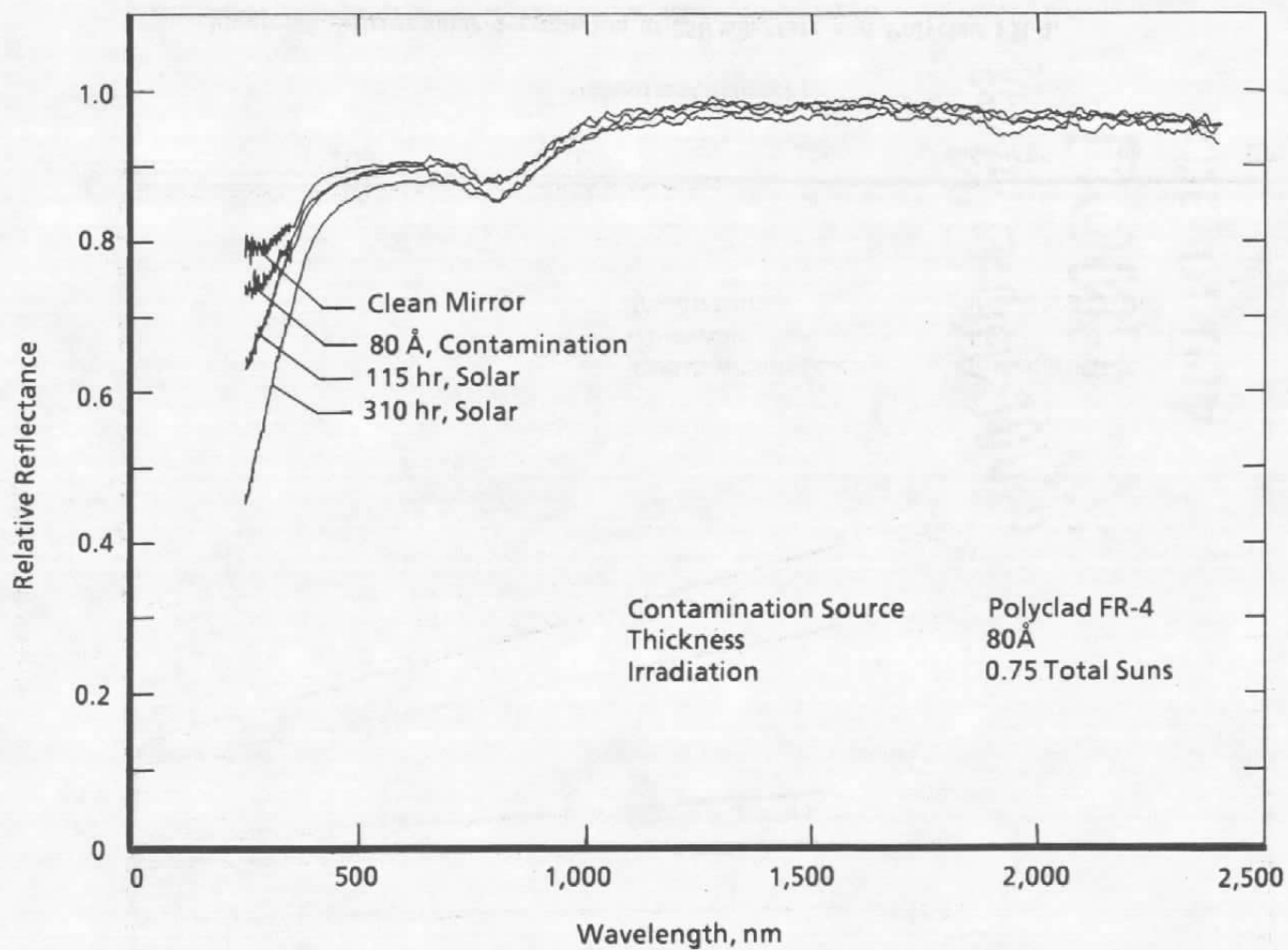Figure 9. Typical QCM-measured contaminant buildup, DC 93-500.
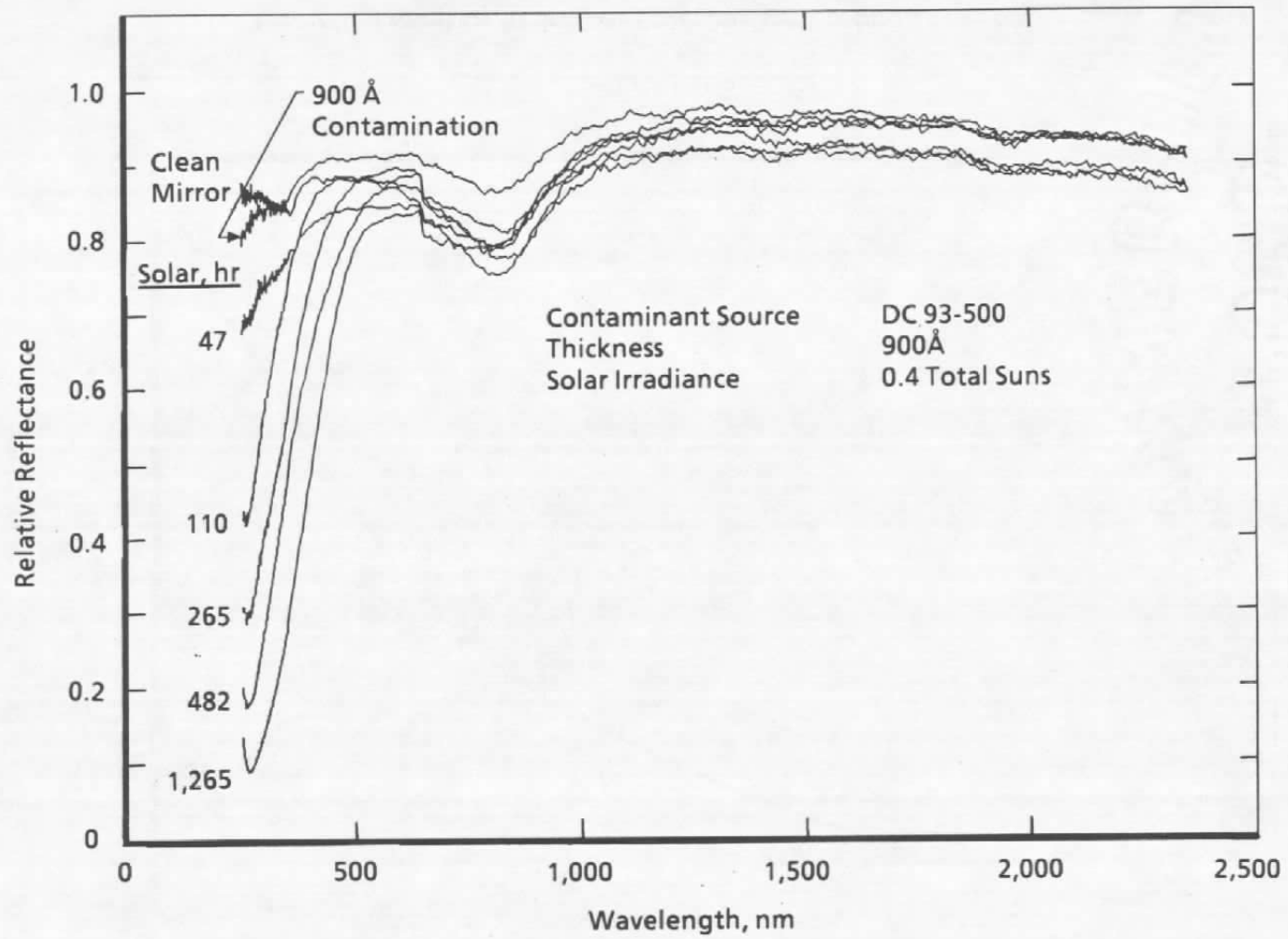
Figure 10. Mirror degradation caused by contaminant and solar Irradiation, DC 93-500.
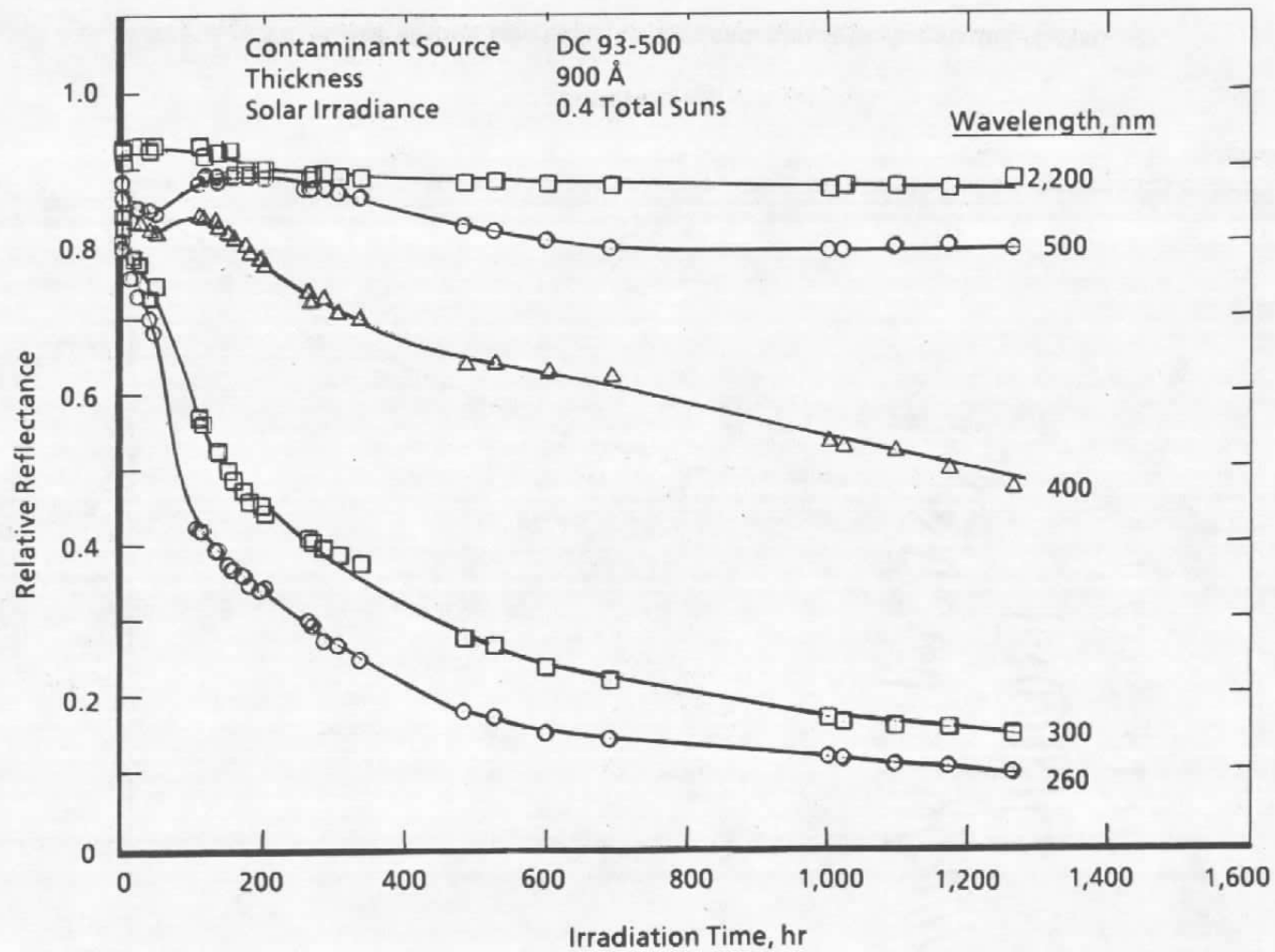
Figure 11. Mirror solar degradation at selected wavelengths, DC 93-500.
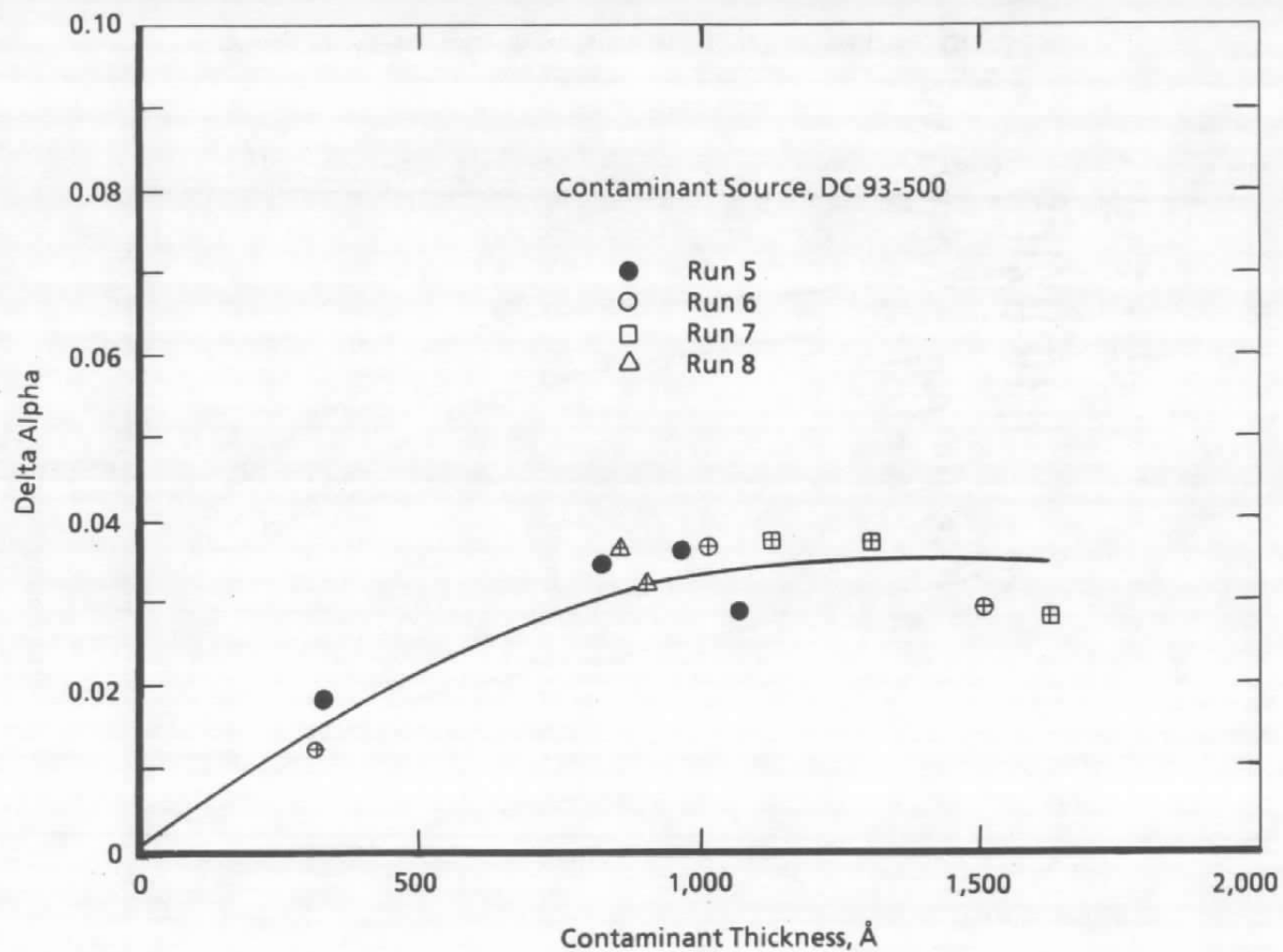
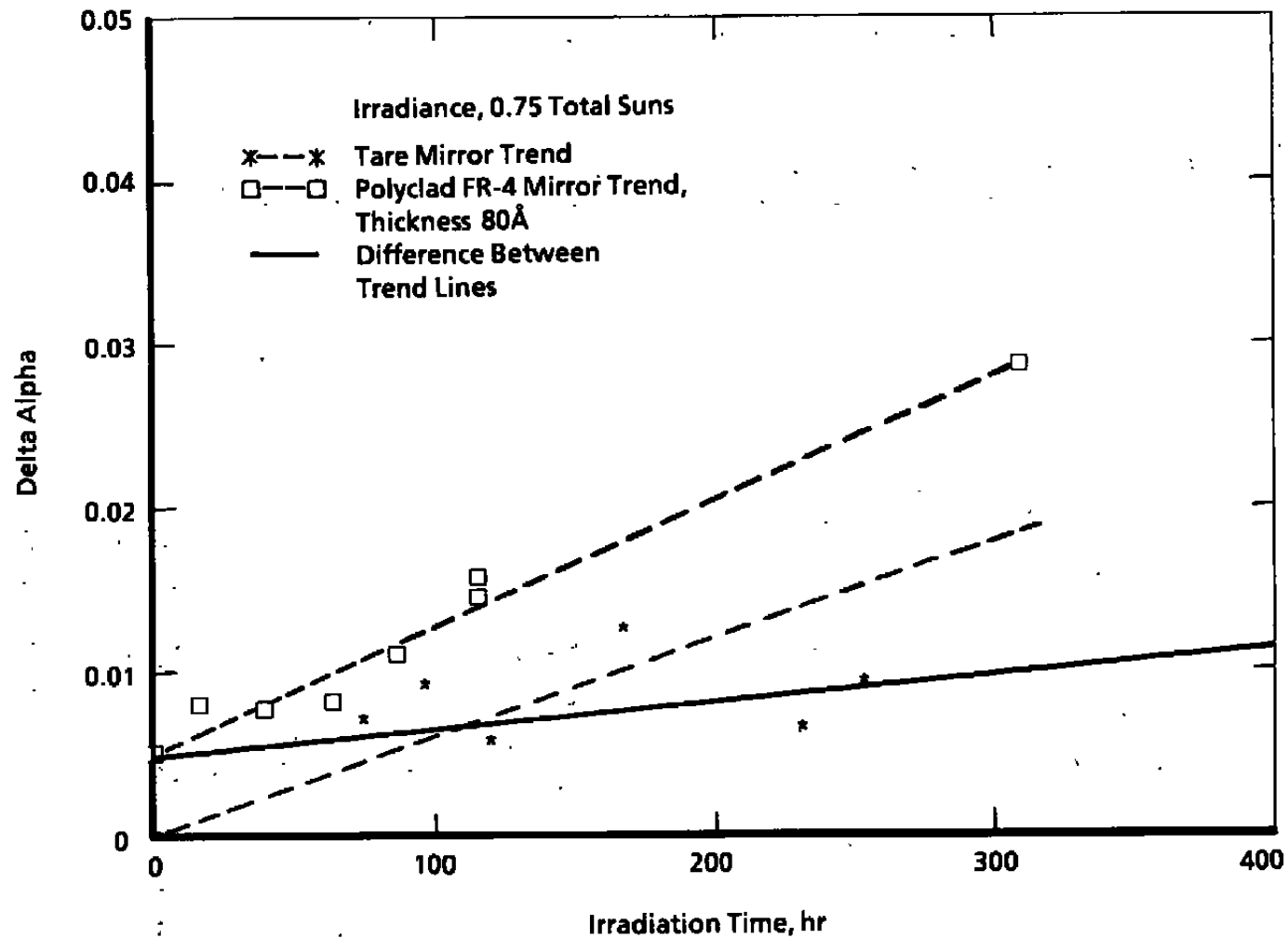Figure 12. Mirror absorptance change with contaminant thickness, DC 93-500.
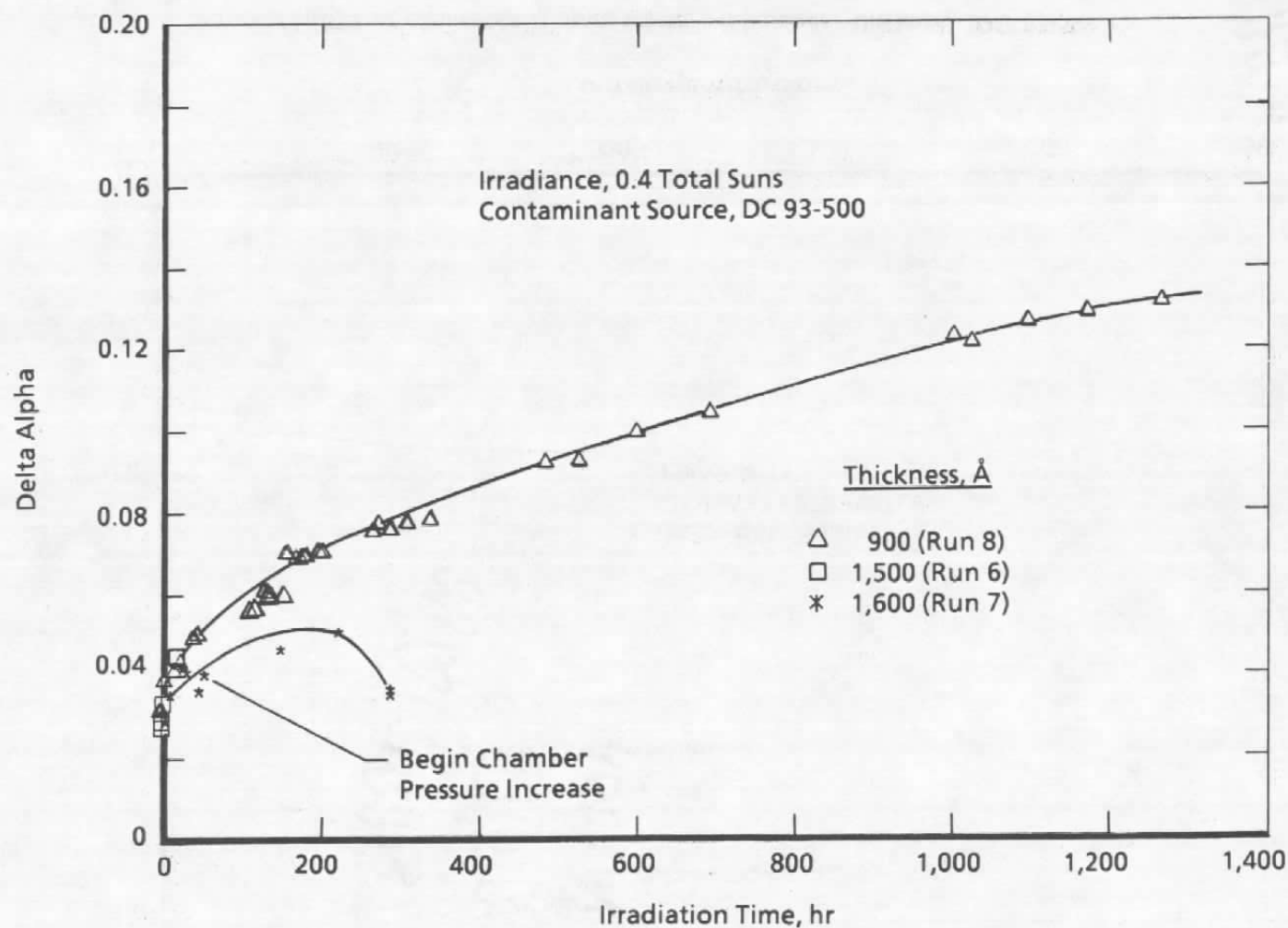
Figure 13. Mirror absorptance change with solar irradiation, DC 93-500.
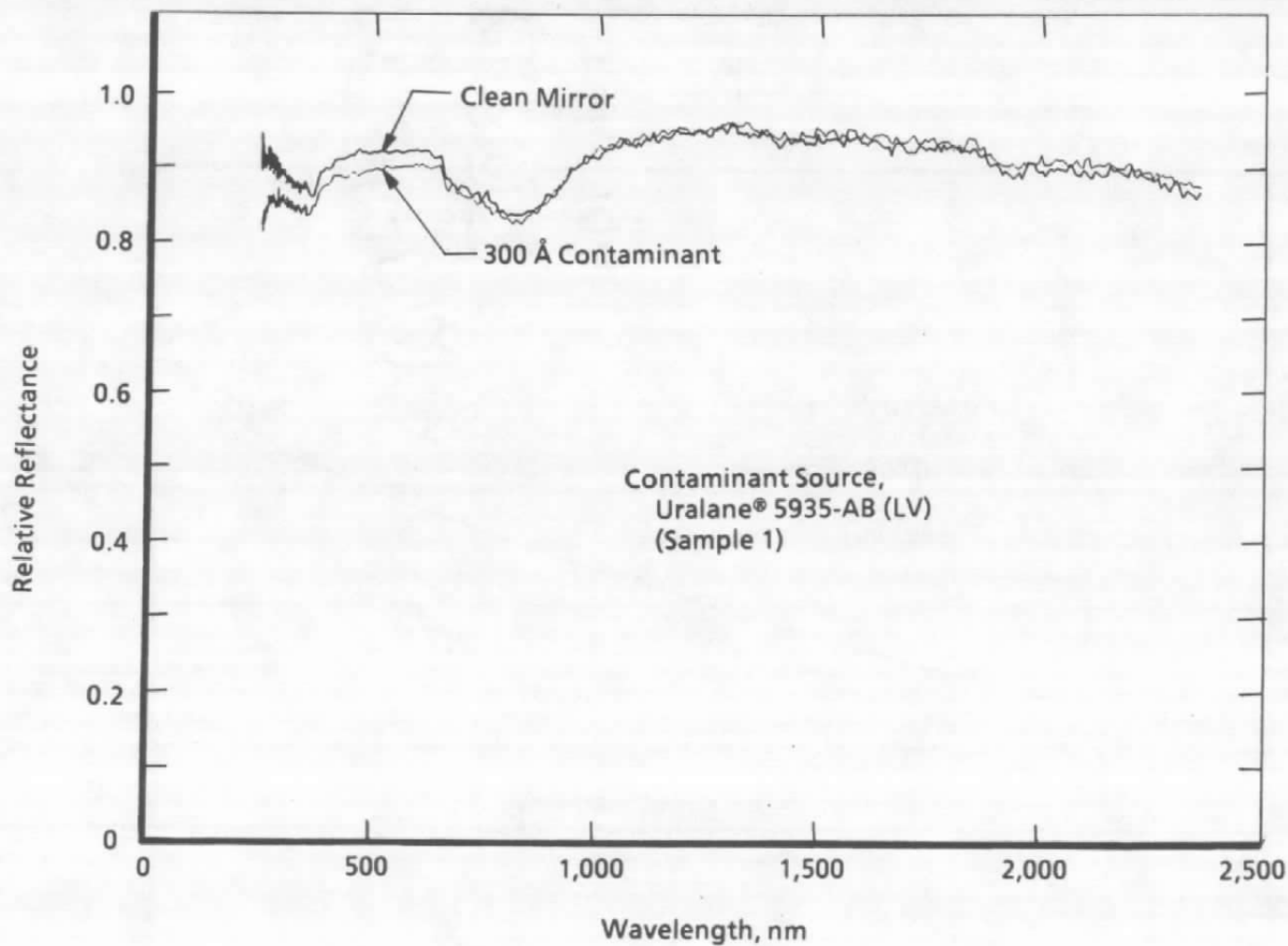
Figure 14. Effect of contaminant upon mirror reflectance, Uralane® 5935-AB(LV).
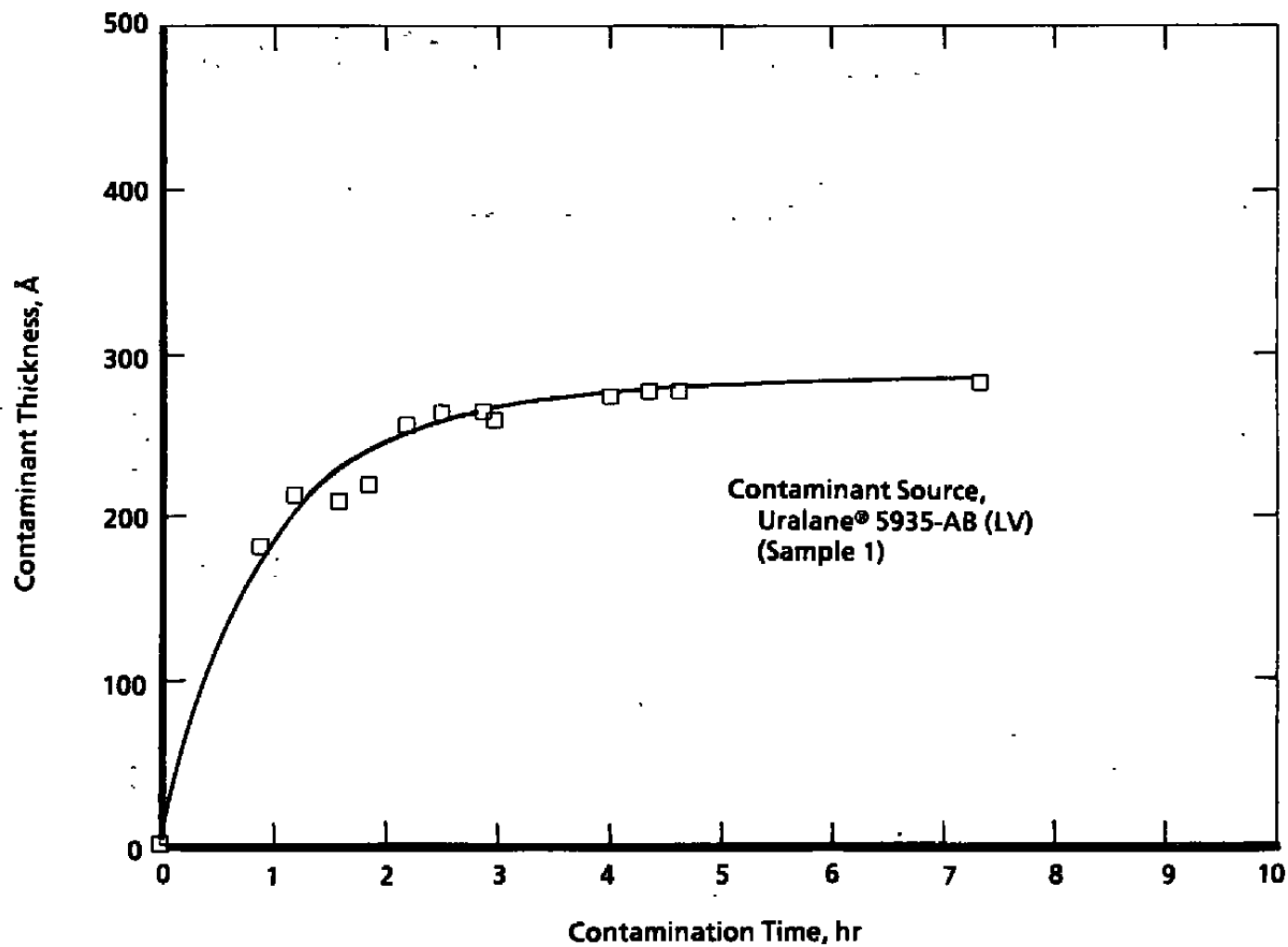
Figure 15. Typical QCM-measured contaminant buildup, Uralane® 5935-AB(LV).
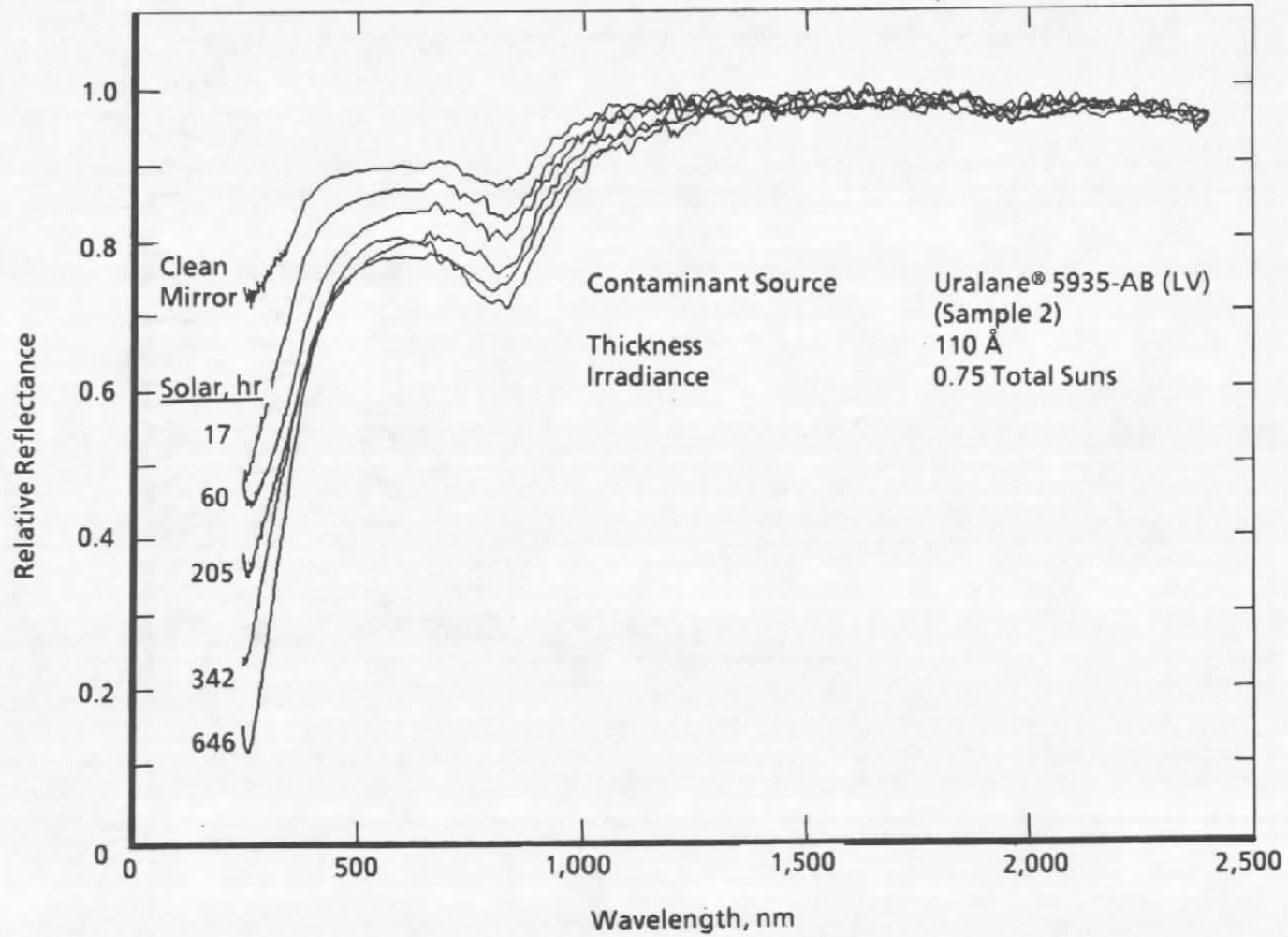
**Figure 16. Mirror degradation with contaminant and solar irradiation, Uralane®
5935-AB(LV).**
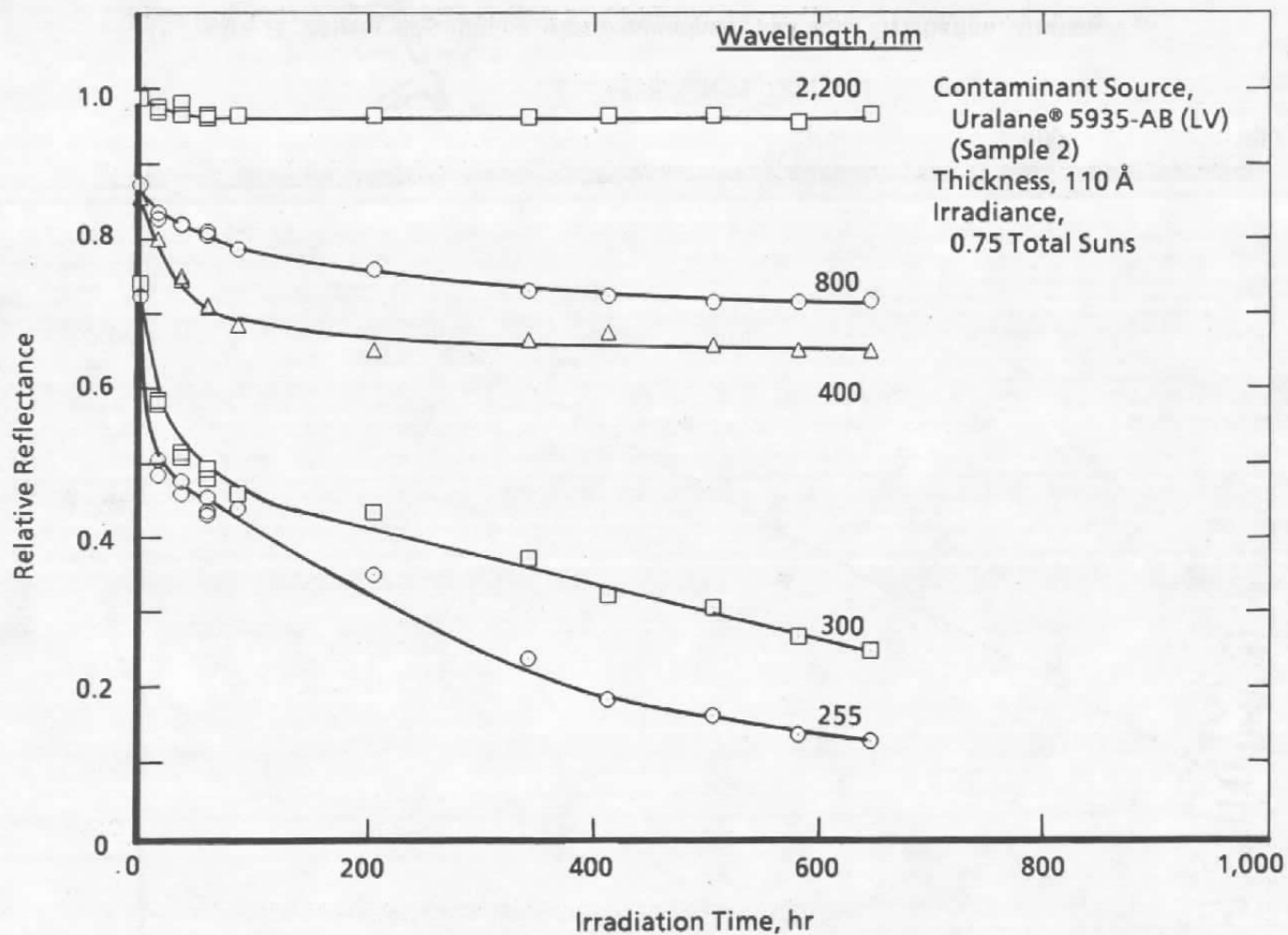
Figure 17. Mirror degradation at selected wavelengths, Uralane® 5935-AB(LV).
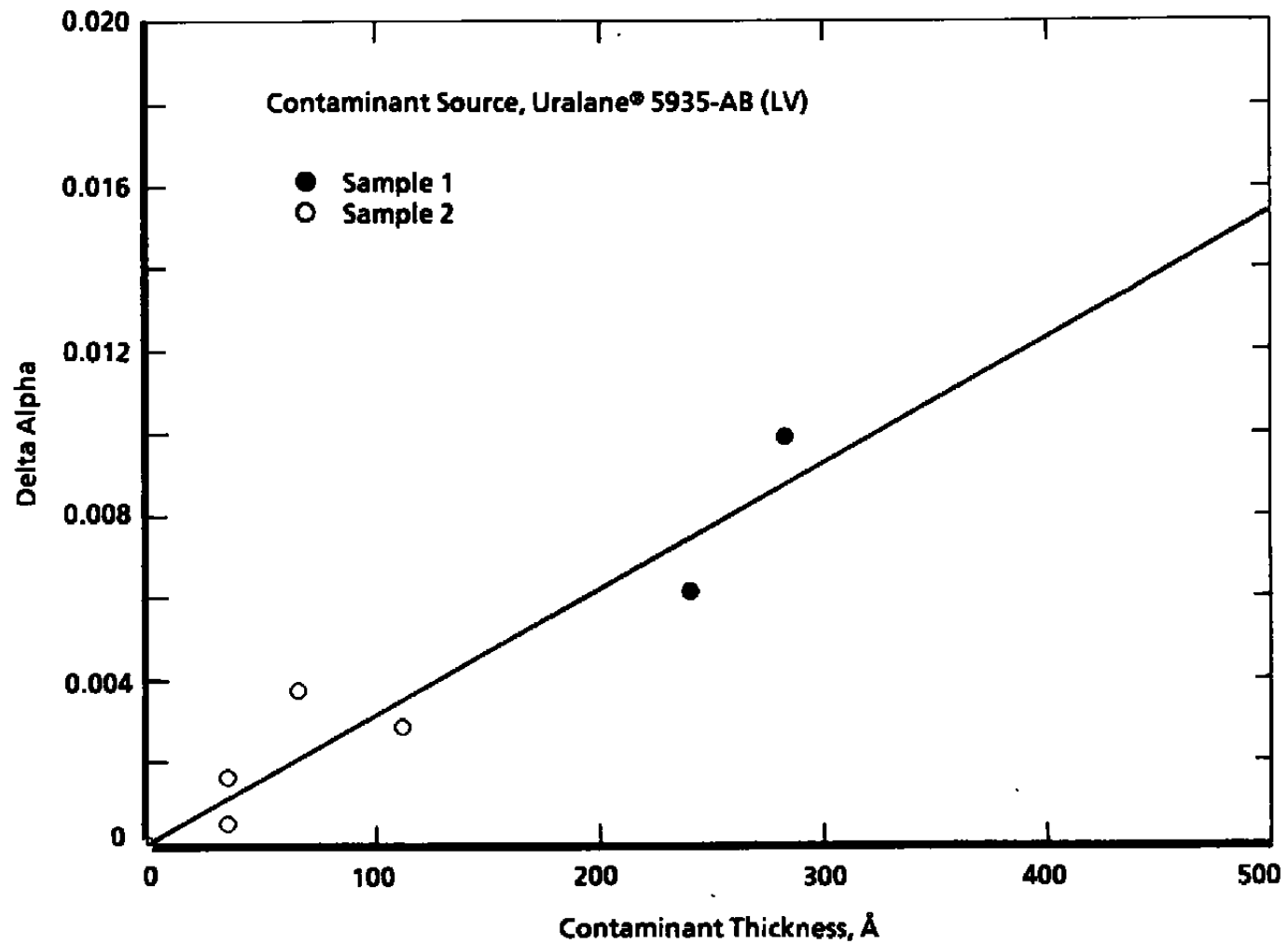
Figure 18. Mirror absorptance change with contaminant thickness, Uralane® 5935-AB(LV).
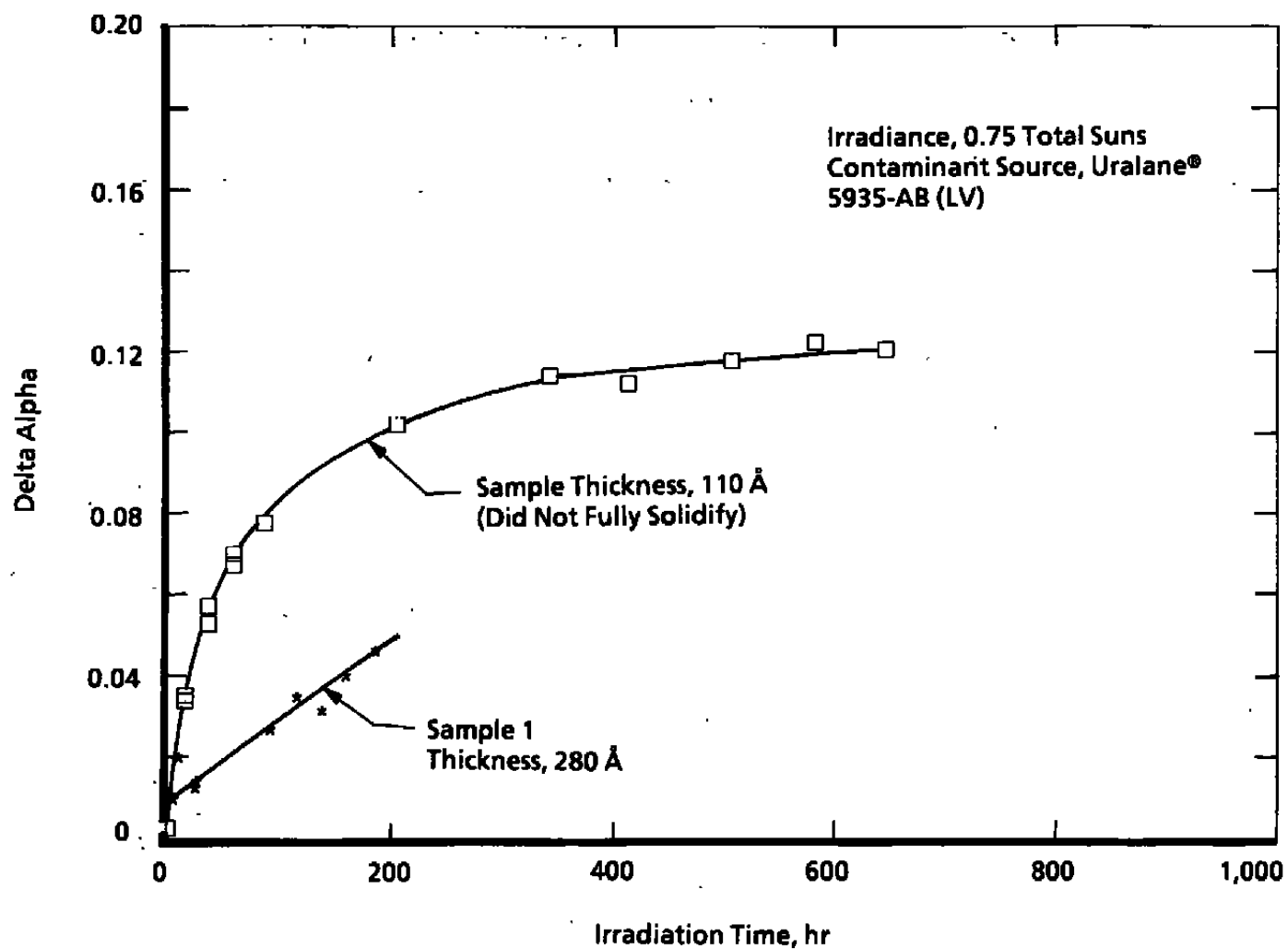
Figure 19. Mirror absorptance change with solar irradiation, Uralane® 5935-AB(LV).
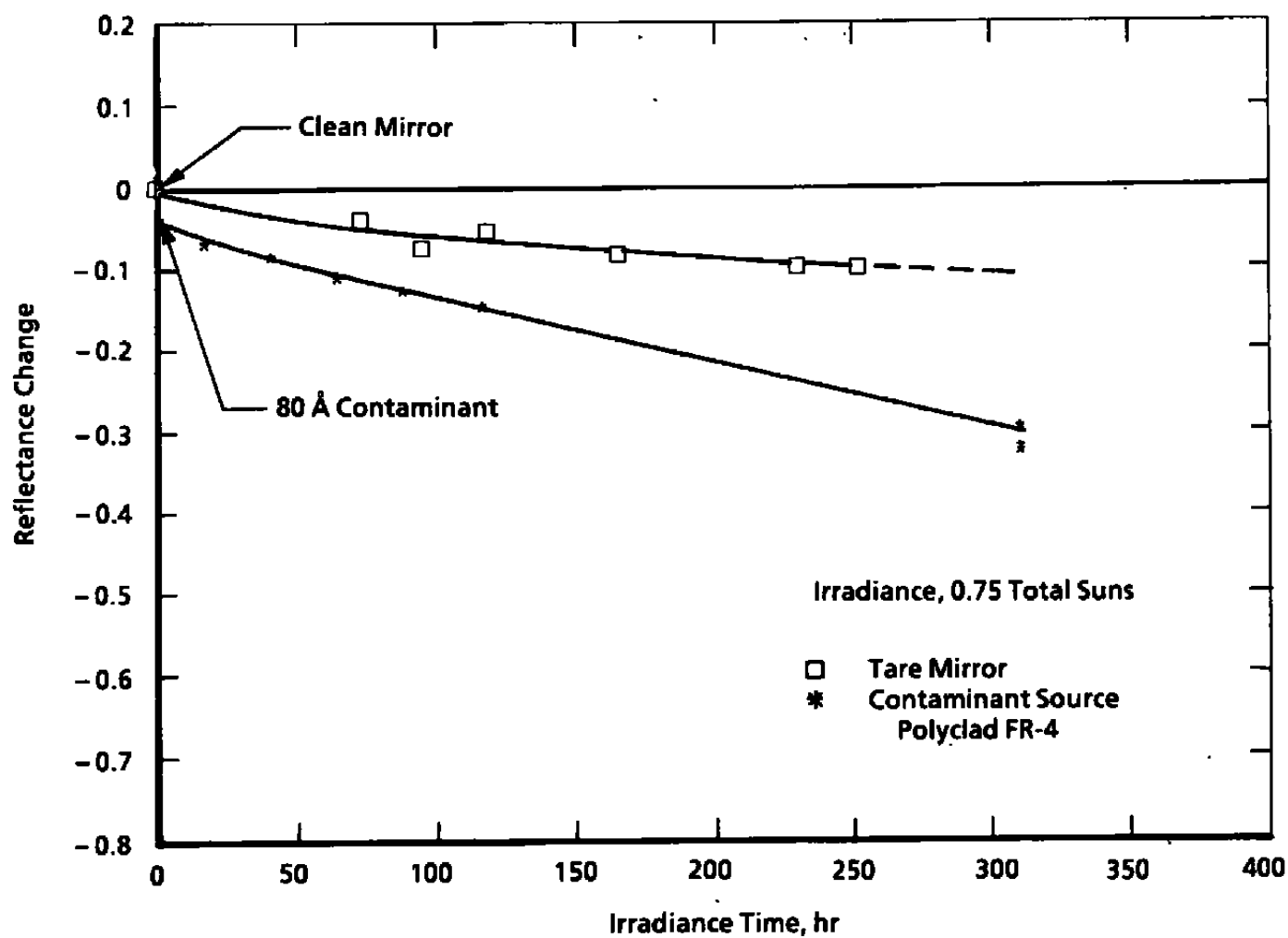
Figure 20. Mirror solar degradation at 250 nm, tare and Polyclad FR-4.

Figure 21. Mirror degradation caused by contaminant and solar irradiation Polyclad FR-4.
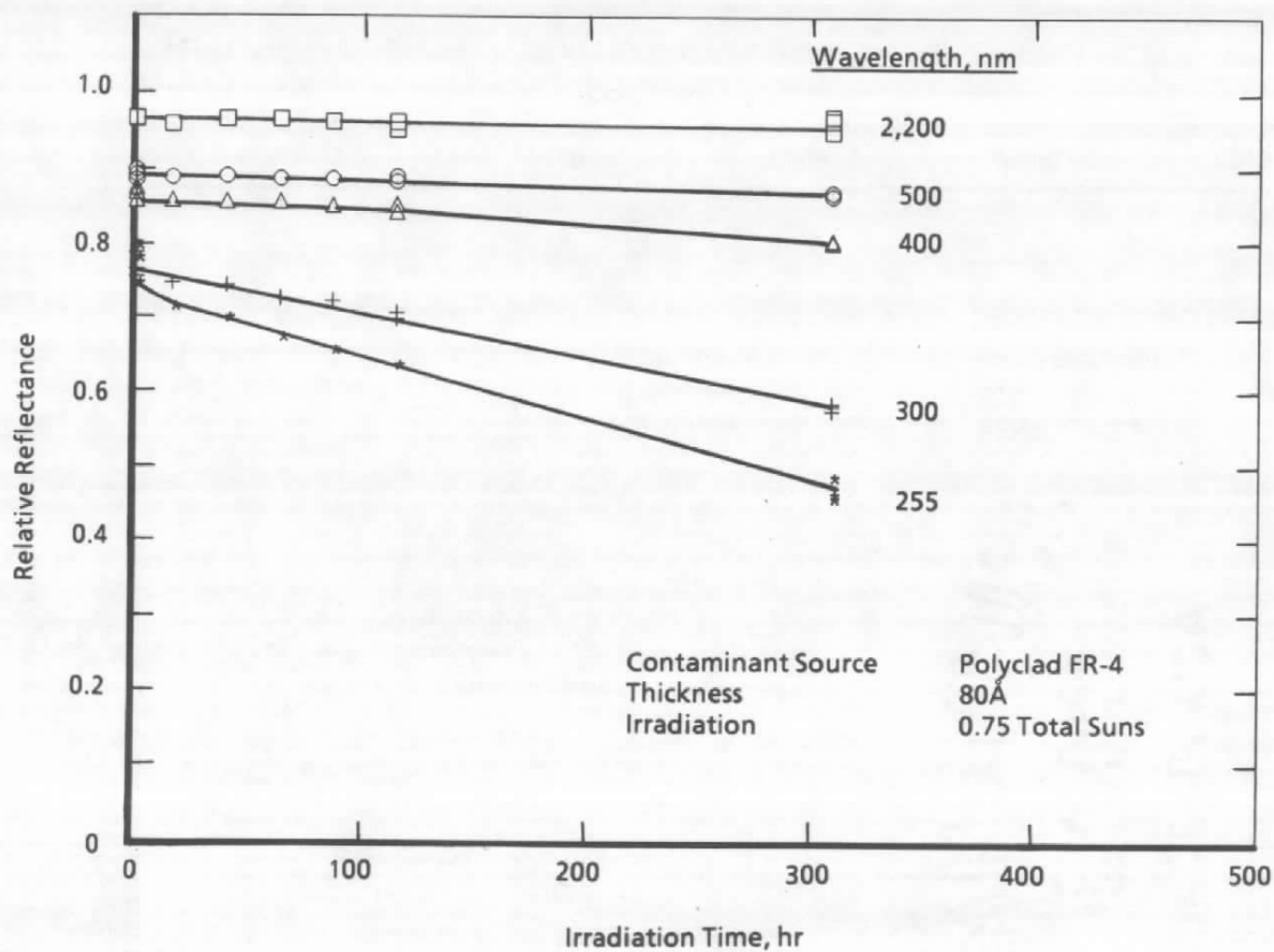
Figure 22. Mirror solar degradation at selected wavelengths, Polyclad FR-4.

Figure 23. Mirror absorptance change with solar irradiation, Polyclad FR-4.
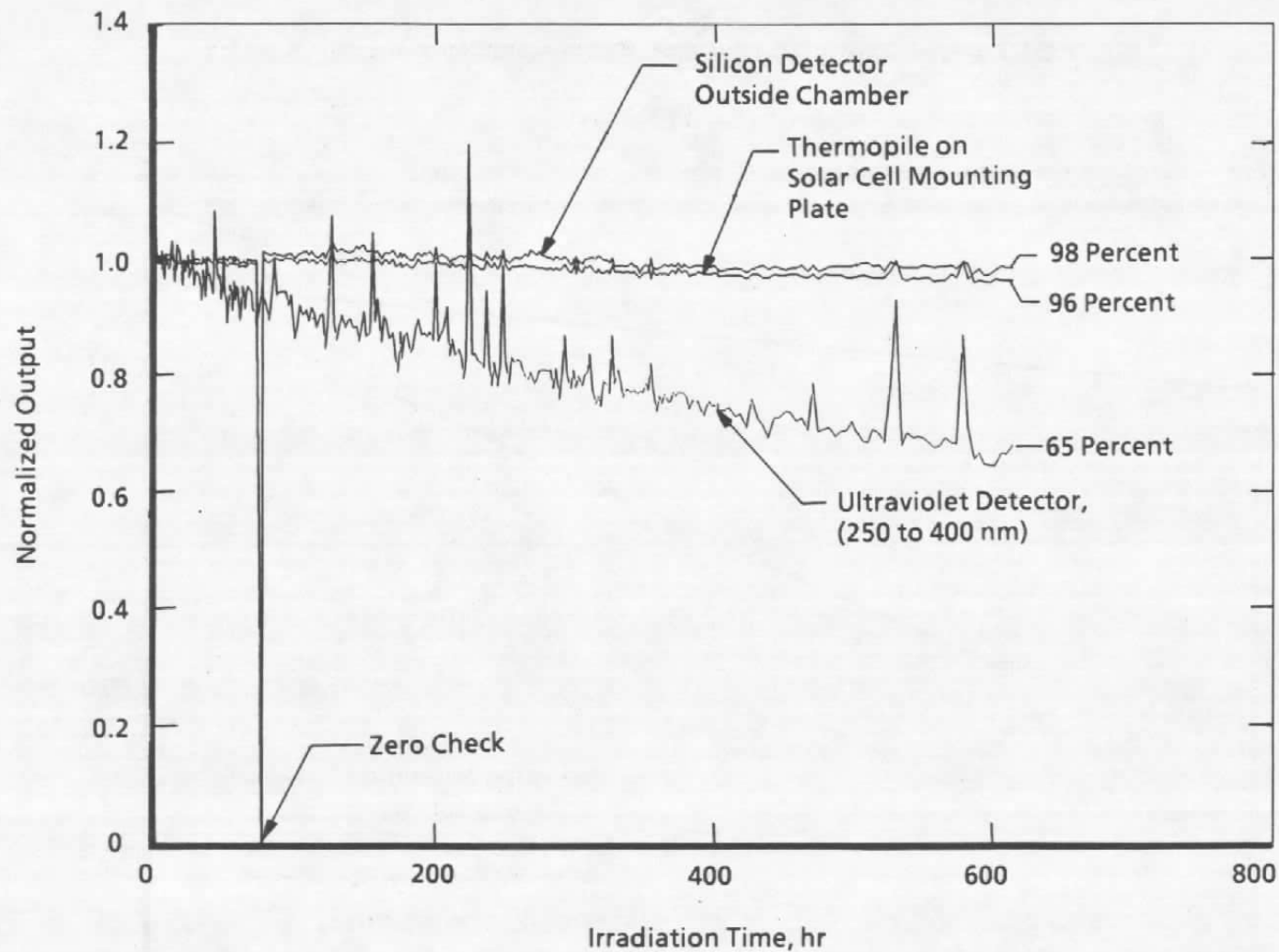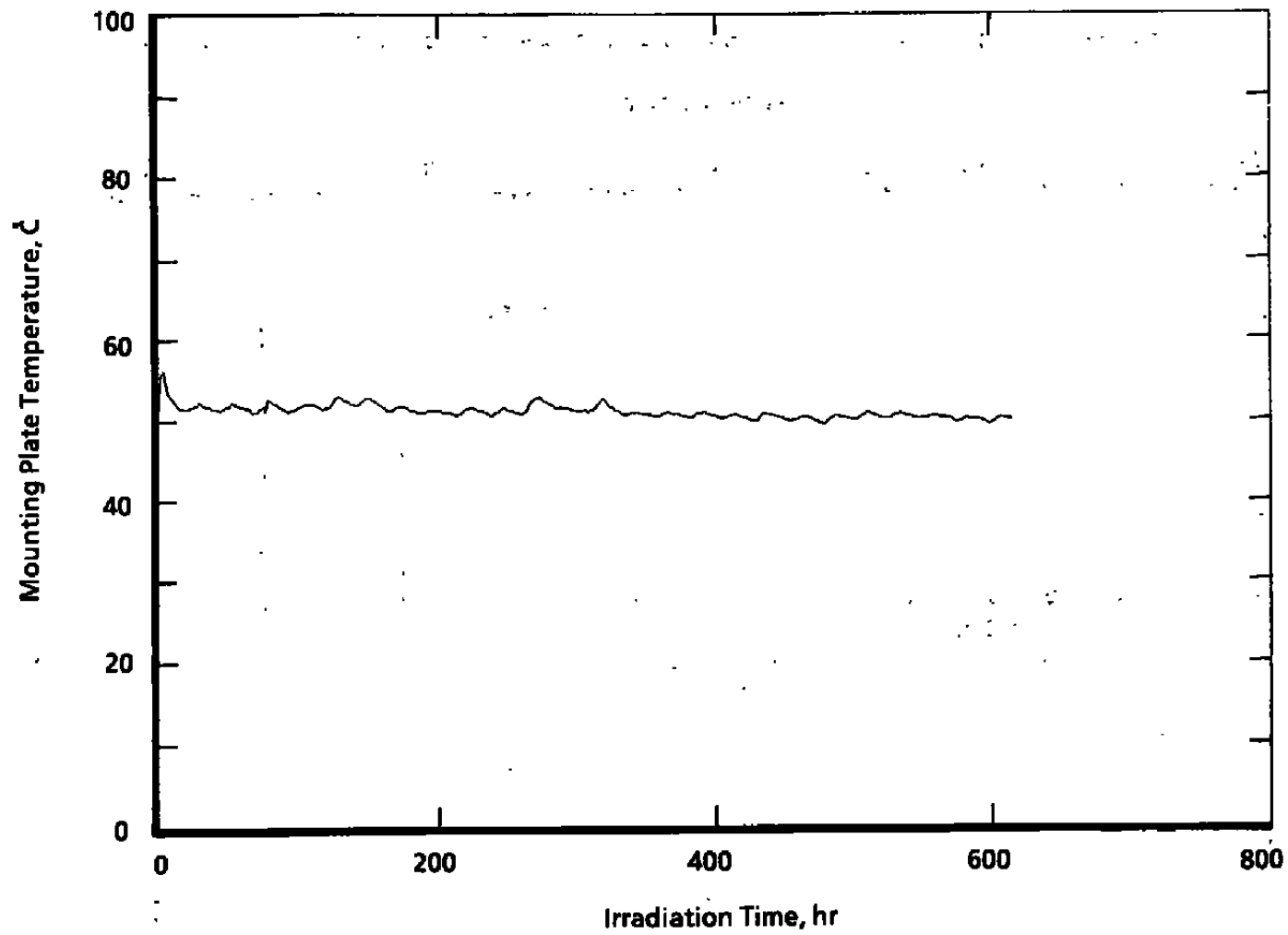
Figure 24. Xenon lamp stability during solar cell test.

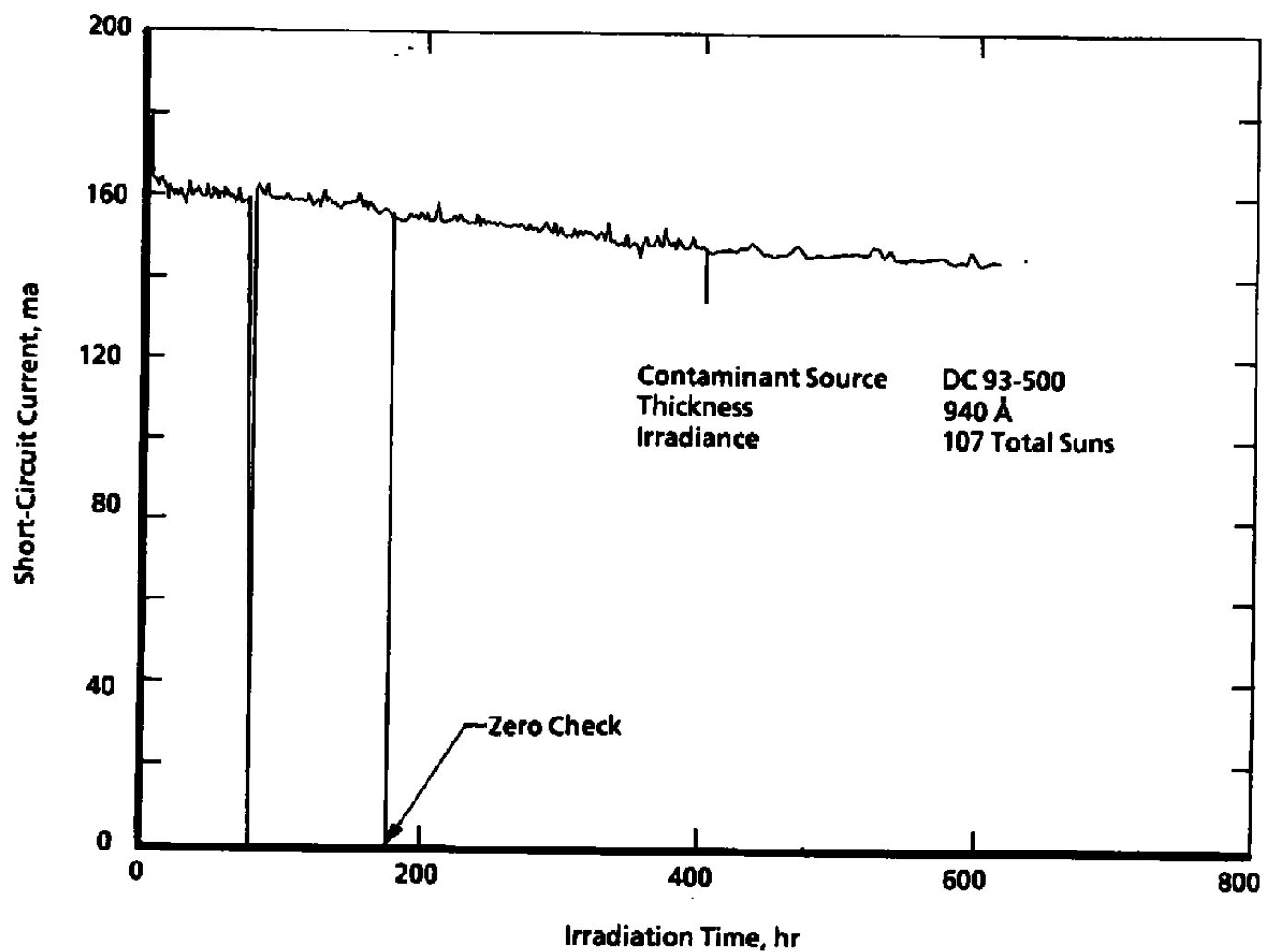Figure 25. Solar cell mounting plate temperature during solar cell test.

Figure 26. Silicon solar cell, S1, degradation with solar irradiation, DC 93-500 contaminant.
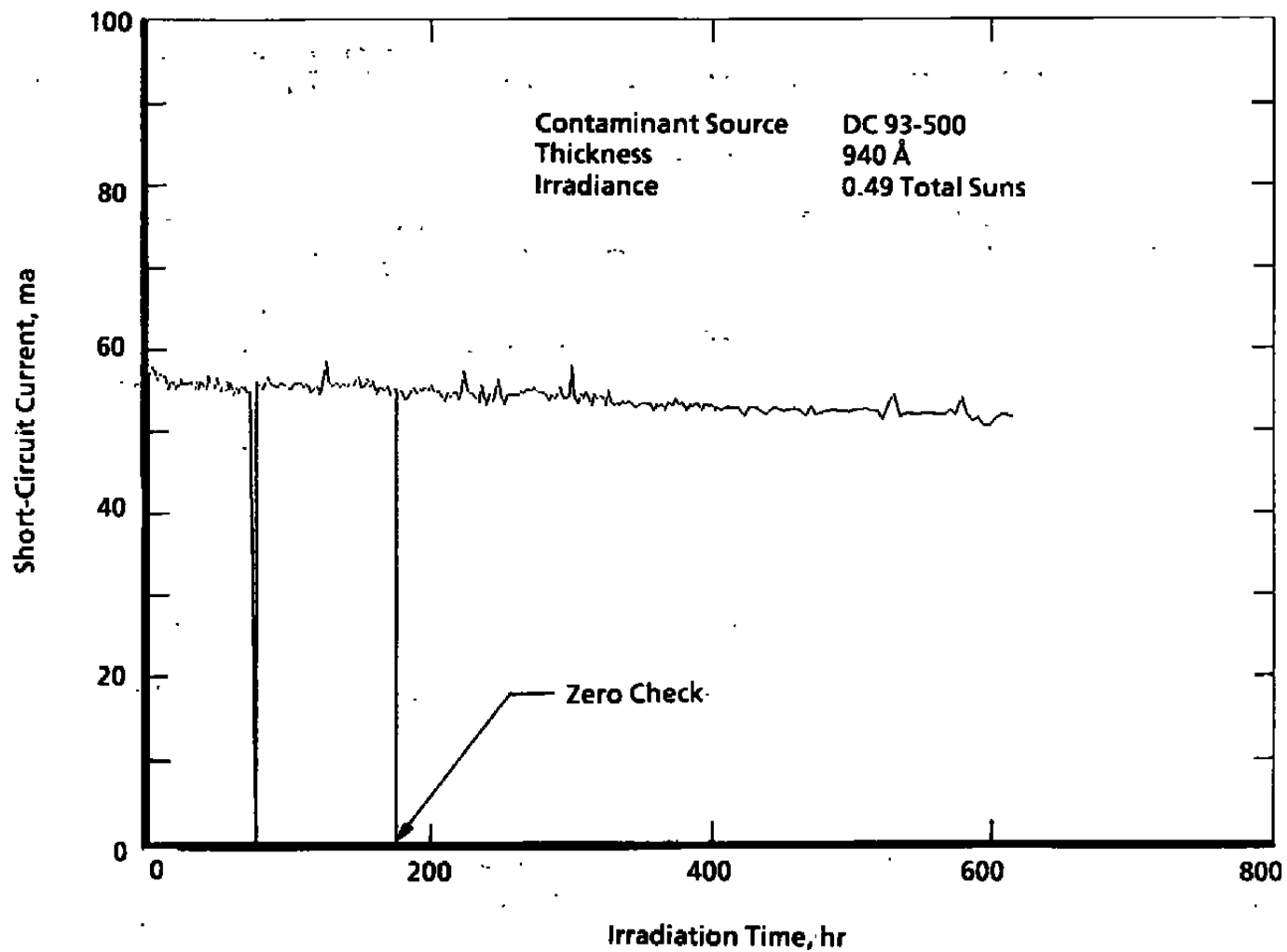
Figure 27. Gallium arsenide solar cell, S3, degradation with solar irradiation, DC 93-500 contaminant.
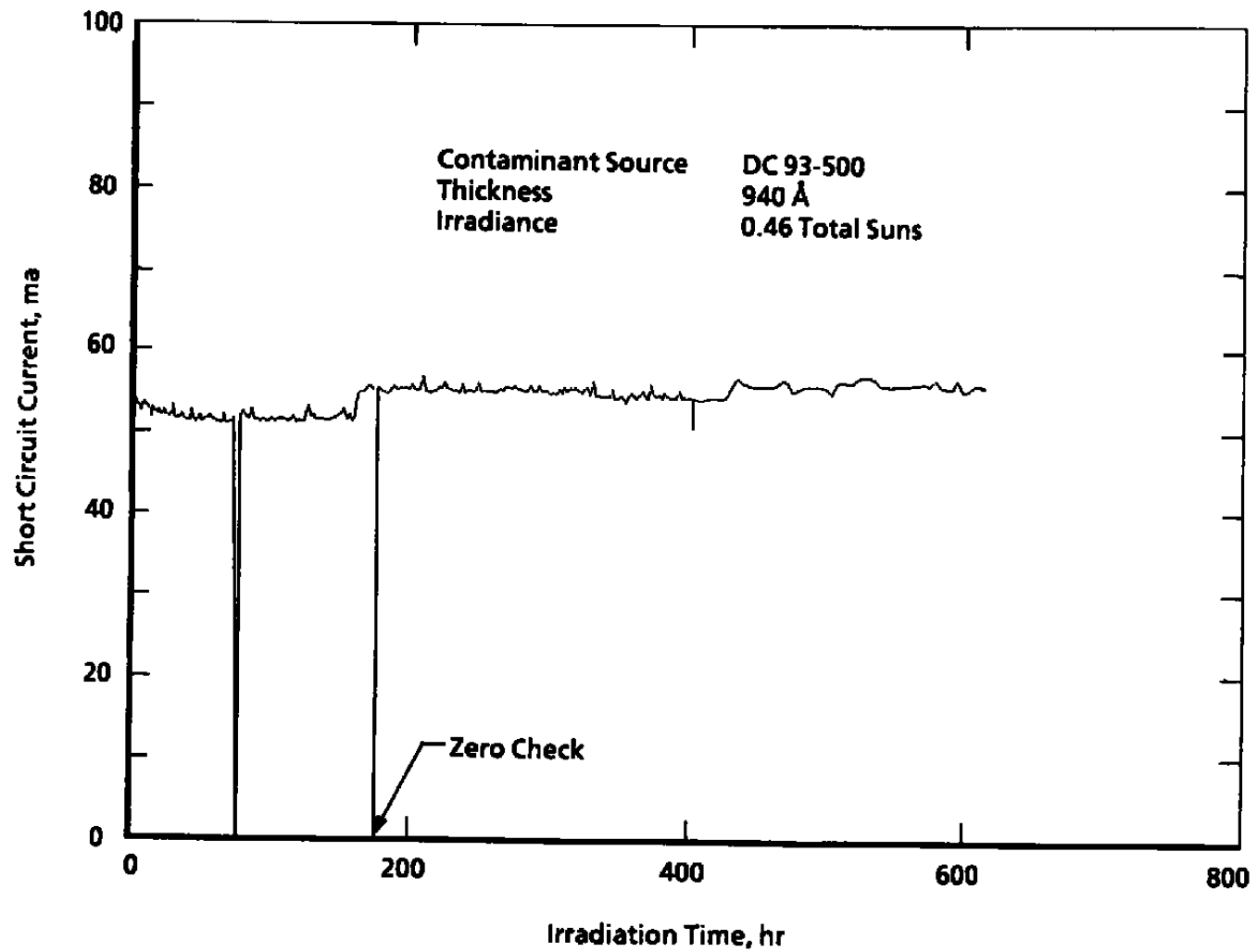
Figure 28. Gallium arsenide solar cell, S2, degradation with solar irradiation, DC 93-500 contaminant.